Enhanced expression of the human *Survival motor neuron 1* gene from a codon-optimised cDNA transgene *in vitro* and *in vivo*

Neda A.M. Nafchi[1]*, Ellie M. Chilcott[1]*, Sharon Brown[2,3], Heidi R. Fuller[2,3], Melissa Bowerman[3,4] and Rafael J. Yáñez-Muñoz[1].

[1] AGCTlab.org, Centre of Gene and Cell Therapy, Centre for Biomedical Sciences, Department of Biological Sciences, School of Life Sciences and Environment, Royal Holloway University of London, TW20 0EX, UK.

[2] School of Pharmacy and Bioengineering, Keele University, Staffordshire, ST5 5BG, UK.

[3] Wolfson Centre for Inherited Neuromuscular Disease, TORCH Building, RJAH Orthopaedic Hospital, Oswestry SY10 7AG, UK.

[4] School of Medicine, Keele University, Staffordshire, ST5 5BG UK.

*These authors contributed equally to this work.

Corresponding author:

Prof. Rafael J. Yáñez-Muñoz

Email: rafael.yanez@royalholloway.ac.uk

Abstract

Spinal muscular atrophy (SMA) is a neuromuscular disease particularly characterised by degeneration of ventral motor neurons. *Survival motor neuron* (*SMN*) *1* gene mutations cause

SMA, and gene addition strategies to replace the faulty *SMN1* copy are a therapeutic option. We have developed a novel, codon-optimised *hSMN1* transgene and produced integration-proficient and integration-deficient lentiviral vectors with cytomegalovirus (CMV), human synapsin (hSYN) or human phosphoglycerate kinase (hPGK) promoters to determine the optimal expression cassette configuration. Integrating, CMV-driven and codon-optimised *hSMN1* lentiviral vectors resulted in the highest production of functional SMN protein *in vitro*. Integration-deficient lentiviral vectors also led to significant expression of the optimised transgene and are expected to be safer than integrating vectors. Lentiviral delivery in culture led to activation of the DNA damage response, in particular elevating levels of phosphorylated ataxia telangiectasia mutated (pATM) and γH2AX, but the optimised *hSMN1* transgene showed some protective effects. Neonatal delivery of adeno-associated viral vector (AAV9) vector encoding the optimised transgene to the $Smn^{2B/-}$ mouse model of SMA resulted in a significant increase of SMN protein levels in liver and spinal cord. This work shows the potential of a novel codon-optimised *hSMN1* transgene as a therapeutic strategy for SMA.

Introduction

Spinal muscular atrophy (SMA) is an autosomal recessive neuromuscular disease chiefly characterised by degeneration of motor neurons from the ventral horn of the spinal cord. *Survival motor neuron* (*SMN*) *1* gene is the SMA-determining gene, being absent in 95% patients and mutated in the remaining 5% (1). *SMN2* is a highly similar gene with only five nucleotide mismatches, which result in 90% truncated transcripts lacking exon 7 (*SMNΔ7*) (2, 3), producing only low levels of SMN protein. *SMN2* copy number is a strict determinant of disease severity, whereby patients with only two copies of the gene present with the severe type I form of SMA while patients with a greater number of *SMN2* copies have less severe symptoms (4-6). Full-length SMN is a ubiquitous and essential cellular protein that has roles in RNA

50 metabolism, cytoskeletal maintenance, transcription, cell signaling and DNA repair (7). For
51 many years, it was thought that motor neurons were the only affected cells, but recent evidence
52 suggests a wide range of systemic pathologies are also caused by low levels of SMN protein.
53 Therefore, an effective and successful therapy for SMA is likely to involve the consideration of
54 SMA as a multi-system disorder (8, 9).
55
56 In the past five years, three therapies for SMA patients have been approved by regulatory
57 bodies: Spinraza, Zolgensma and Evrysdi, the first two of which are genetic therapies. Spinraza
58 is an antisense oligonucleotide that increases the level of full-length SMN protein by binding and
59 altering the splicing of *SMN2* pre-mRNA (10), enhancing the inclusion of exon 7 (11).
60 Zolgensma is an adeno-associated viral vector of serotype 9 (AAV9) vector containing the
61 cDNA of the human *SMN1* gene under the control of the cytomegalovirus enhancer/chicken-β-
62 actin-hybrid promoter (12). Evrysdi is a small molecule that modulates *SMN2* RNA splicing by
63 binding to two unique sites in *SMN2* pre-mRNA: 5′ splice site of intron 7 and an exonic splicing
64 enhancer 2 in exon 7, therefore promoting inclusion of exon 7 (13). Evrysdi is an oral medicine
65 expected to be taken for the duration of the individual's life (13), while Spinraza requires
66 repeated delivery through intrathecal injections and Zolgensma is a one-off intravenous infusion.
67
68 Gene therapy is a technology that allows the modification of gene expression with one possible
69 strategy being the introduction of transgenes for therapeutic purposes. In this context, the
70 efficient delivery of therapeutic genes, or other gene therapy agents, is a critical requirement for
71 the development of an effective treatment. Vectors derived from lentiviruses have proven to be
72 efficient gene delivery vehicles as they integrate into the host's chromosomes and show
73 continued expression for a long time (14). They also have a relatively large cloning capacity,
74 which is sufficient for most clinical purposes (15, 16). Lentiviral vectors can transduce different
75 types of cells, including quiescent cells, have low immunogenicity upon *in vivo* administration,

76 lead to stable gene expression and can be pseudotyped with alternative envelopes to alter
77 vector tropism (17).
78
79 Due to their unique advantages, lentiviral vectors are important gene delivery systems for
80 research and clinical applications (16). Lentiviral vectors have been utilised to treat symptoms in
81 several animal models, such as X-linked severe combined immunodeficiency (SCID-X1) (18), β-
82 thalassemia (19), Wiskott-Aldrich syndrome (20), metachromatic leukodystrophy (21),
83 haemophilia (22), Fanconi anaemia (23) and liver disease (24), as well as being used in clinical
84 applications (25-27). Although the integrative nature of lentiviral vectors provides long-term
85 transgene expression, integration events carry the risk of insertional mutagenesis (28-30).
86 Intensive study of the genome and analysis of integration strategies of lentiviral vectors has led
87 to the development of a number of strategies to minimise these risks. These include the use of
88 viral vectors with a safer integration pattern, the utilisation of self-inactivating vectors and the
89 design of integration-deficient lentiviral vectors (IDLVs). IDLVs are non-integrative due to an
90 engineered class I mutation in the viral *integrase* gene, most commonly involving an amino acid
91 change at position D64 within the catalytic core domain (31).
92
93 Here, we show the development of an integration-deficient lentiviral system expressing a novel,
94 sequence ("codon")-optimised cDNA transgene, *Co-hSMN1*, which leads to effective SMN
95 production in primary cultures and rescue of nuclear gems, distinct and punctate nuclear bodies
96 where the SMN protein localises in high concentrations. Rescue of SMN production was also
97 seen in an SMA type I induced pluripotent stem cell (iPSC)-derived motor neuron (MN) model.
98 *In vivo* data showed that an AAV9 vector expressing this transgene could strongly restore SMN
99 protein production in the $Smn^{2B/-}$ SMA mouse model (32). We also found that untreated SMA
100 cells exhibit molecular signatures of DNA damage with prominent γH2AX foci and a trend for
101 increased pATM expression. Notably, IDLV_*Co-hSMN1* was able to reverse an initial spike in

102 pATM signaling, suggesting some protective effect. Together, these data point to novel benefits
103 of gene therapy for SMA, and importantly, highlight an alternative transgene and delivery
104 system.
105

106 Materials and methods

107 *Optimisation of hSMN1 sequence*

108 The wild-type cDNA sequence of the human *SMN1* transcript was codon-optimised using
109 custom services provided by GeneArt/ThermoFisher Scientific to generate *Co-hSMN1*. The
110 GeneArt algorithm identifies and optimises a variety of factors relevant to different stages of
111 protein production, such as codon adaptation, mRNA stability, and various *cis* elements in
112 transcription and translation to achieve the most efficient expression. This transgene was then
113 cloned into lentiviral and AAV transfer plasmid using standard molecular biology procedures.
114

115 *Fibroblast cell culture*

116 Low passage, primary human fibroblasts from wild-type (GM04603) and SMA type I (GM00232)
117 donors were obtained from Coriell Institute for Medical Research and used to assess overall
118 lentiviral transduction efficiency, γH2AX and caspase 3 foci, and ATM and pATM levels. Similar
119 wild-type and SMA type I fibroblast cell lines were also obtained from E. Tizzano (33) and used
120 to assess restoration of gems following transduction. All fibroblasts were cultured in 65%
121 DMEM+Glutamax, 21% M199, 10% FBS, 10 ng/ml FGF2, 25 ng/ml EGF and 1 µg/ml
122 gentamicin.
123

124 *Isolation and culture of E18 mouse cortical neurons*

125 Preparation of primary cortical cultures from E18 mouse embryos followed the protocol
126 described in Lu-Nguyen *et al* (34).
127

128 *Preparation of embryonic rat motor neuron primary cultures*

129 The isolation and culture of primary rat motor neurons was achieved by following the protocol
130 previously described in Peluffo et al (35).
131

132 *iPSC culture and motor neuron differentiation*

133 Six iPSC lines were used in this project; three wild-type (4603, derived in house from GM04603
134 fibroblasts (33); 19-9-7T, from WiCell and AD3-CL1, gifted by Majlinda Lako) and three SMA
135 type I (SMA-19, gifted by Majlinda Lako; CS13iSMAI-nxx and CS32iSMAI-nxx, obtained from
136 Cedars-Sinai). Undifferentiated iPSCs were seeded at a density of 20,000 cells/cm^2 onto
137 Matrigel-coated cultureware in mTeSR™1 or mTeSR™ Plus media for general growth.
138

139 iPSCs were grown until 90% confluent in 6 well plates then clump passaged with 0.5 mM EDTA
140 to Matrigel-coated 10 cm dishes until 60-70% confluent. A protocol adapted from Maury et al
141 (36) was used to differentiate iPSCs into MNs. Basal medium (1X DMEM/F12, 1X Neurobasal,
142 1X B27, 1X N2, 1X antibiotic-antimycotic, 1X *β*-mercaptoethanol and 0.5 μM ascorbic acid) was
143 used throughout the 28-day protocol. Basal medium was supplemented at specific stages with
144 additional compounds: 3 μM Chir99021 (days 0-3), 1 μM Compound C (days 0-3), 1 μM retinoic
145 acid (day 3+), 500 nM SAG (day 3+), 0.5 μg/ml laminin (day 16+), 10 ng/ml each of IGF1,
146 CNTF, BDNF, GDNF (all day 16+) and 10 μM DAPT (days 16-23). Single cell passaging on
147 days 9, 13 (1:3 split ratio) and 16 (at appropriate density for final assay) was performed using
148 Accutase and cells were re-seeded onto Matrigel-coated cultureware in the presence of 10 μM
149 ROCK inhibitor for 24 hours.

150

151 *Viral vector production*

152 A 3rd generation, transient transfection system was used to generate self-inactivating HIV-1-
153 based lentiviral vectors by calcium phosphate co-transfection of HEK293T/17 cells with
154 pMDLg/pRRE or pMDLg/pRRE_intD64V (for integrating and non-integrating vectors,
155 respectively), pRSV_REV, pMD2_VSV-G and a transfer plasmid containing the promoter of
156 interest and either *hSMN1*, *Co-hSMN1* or *eGFP* at a 1:1:1:2 ratio, respectively. Supernatants
157 were harvested at 48- and 72-hours post-transfection and lentiviral vectors were concentrated
158 by ultracentrifugation. Vectors were titrated by qPCR and where possible, by flow cytometry
159 (31).

160

161 AAV_CAG_*Co-hSMN1* and AAV_CAG_*eGFP* vectors were commercially produced by Atlantic
162 Gene Therapies (France) and were titrated by qPCR against the inverted terminal repeats
163 (ITRs).

164

165 *Viral transduction in cell culture*

166 For transduction of cell lines and primary fibroblasts, cells were seeded in appropriate media 24
167 hours prior to transduction. Lentiviral vectors were diluted in fresh media at the desired qPCR
168 MOI then added to cells in the minimum volume needed to cover cells. 1 hour after transduction,
169 media was topped up to an appropriate volume. All cells were incubated for 72-hours before
170 analysis. Fibroblasts were transduced in the presence of 2 µg/ml polybrene. iPSC-derived MNs
171 were transduced at day 28 of differentiation to ensure maturity of cells.

172

173 Transduction of primary motor neurons was carried out 2 hours post-seeding, while for primary
174 cortical neurons it was three weeks post-seeding. Lentiviral vectors were diluted in conditioned
175 media at the desired qPCR MOI. Analyses were performed three days post-transduction.
176

177 *Viral transduction* in vivo

178 Single-stranded AAV9 vectors (AAV9_CAG_*Co-hSMN1* & AAV9_CAG_*eGFP*) were
179 administered intravenously through the facial vein to post-natal day (P) 0 *Smn*$^{2B/-}$ SMA mice at a
180 dose of 8E10 vg/pup. Liver and spinal cord were harvested at P18 from untreated *Smn*$^{2B/-}$ mice
181 (n=6), *Smn*$^{2B/-}$ mice treated with AAV9_CAG_*eGFP* (n=5) or AAV9_CAG_*Co-hSMN1* (n=5) and
182 age-matched wild-type controls (n=4). At P18 there are overt symptoms in untreated *Smn*$^{2B/-}$
183 mice.
184

185 Experimental procedures were authorized and approved by the Keele University Animal Welfare
186 Ethical Review Body (AWERB) and UK Home Office (Project Licence P99AB3B95) in
187 accordance with the Animals (Scientific Procedures) Act 1986.
188

189 *RT-PCR*

190 An RT-PCR was performed using cDNA extracted from SMA iPSC MNs to identify the origins of
191 *SMN* transcripts. The primers used to amplify a region between exons 6-8 of the *SMN* genes,
192 plus β-actin and GAPDH as housekeeping genes were as follows: Exon6_F
193 CTCCCATATGTCCAGATTCTCTTG, Exon8_R CTACAACACCCTTCTCACAG, β-actin_F
194 TCACCCACACTGTGCCCATCTACGA, β-actin_R CAGCGGAACCGCTCATTGCCAATGG,
195 189_mGapdhex4_Fw AAAGGGTCATCATCTCCGCC, 190_mGapdhex4-5_Rv

196 ACTGTGGTCATGAGCCCTTC. *SMN* RT-PCR amplicons were digested with *Dde*I to reveal *FL-*
197 *SMN1* (504bp), *FL-SMN2* (382+122bp) and *SMN2Δ7* (328+122bp) transcripts.
198

199 *Immunofluorescence*

200 Fibroblasts were fixed with 4% PFA before being concurrently permeabilised and blocked in 5%
201 normal goat serum in PBS with 0.25% Triton X-100. Primary and secondary antibodies were
202 incubated with samples overnight at 4°C or 1 hour at room temperature, respectively. iPSC MNs
203 were seeded at a density of 25,000 cells on day 16 of differentiation onto 13 mm coverslips
204 coated with 15 µg/ml poly-ornithine and Matrigel. 4% PFA and 5% normal goat serum in PBS
205 with 0.25% Triton X-100 were used to fix, permeabilise and block coverslips before antibody
206 incubation at room temperature for both primary (2 hours) and secondary (1 hour). All cells were
207 counterstained with 1 µg/ml DAPI, mounted using Fluoromount™ Aqueous mounting medium
208 then imaged using a Zeiss Axio Observer D1 fluorescent microscope (Germany).
209

210 Primary antibodies: anti-gemin2 (Abcam, ab6084, 2.5 µg/ml), anti-SMN (BD Biosciences,
211 610646, 0.6 µg/ml), anti-OLIG2 (Santa Cruz, sc-515947, 2 µg/ml), anti-SMI-32 (Biolegend,
212 801701, 10 µg/ml), anti-βIII-tubulin (Sigma, T2200, 10 µg/ml), anti-choline acetyltransferase
213 (Abcam, ab181023, 5.4 µg/ml), anti-HB9 (DSHB, 81.5c10, 1:50). Secondary antibodies: goat
214 anti-mouse IgG Alexa Fluor 488 (Invitrogen, A-11001, 2 µg/ml), goat anti-mouse IgG Alexa
215 Fluor 555 (Invitrogen, A-21424, 2 µg/ml), goat anti-rabbit IgG Alexa Fluor 488 (Invitrogen, A-
216 11034, 2 µg/ml).
217

218 *Measurement of SMN intensity by immunofluorescence*

219 Analyses of all samples was performed blind to vector type, gene of interest and MOI.
220 Fluorescence pixel intensities (background corrected) were measured in a region of interest
221 around the motor neuron cell body and are expressed as arbitrary units (a.u.) per μm^2.
222

223 *Western blotting*

224 Cultured cells were lysed in RIPA buffer supplemented with Halt Protease Inhibitor Cocktail and
225 Phosphatase Inhibitor Cocktail 3 and the concentration of resulting protein lysates was
226 determined using the Bio-Rad DC protein assay according to manufacturer's instructions. SMN
227 western blots used 4-15% Tris-Glycine gels and PageRuler™ Plus Prestained Protein Ladder,
228 whilst ATM and phosphorylated ATM western blots used NuPAGE™ 3-8% Tris-Acetate gels
229 and HiMark™ Pre-stained protein standard. Western blots containing samples from iPSC MNs
230 were subjected to total protein staining immediately after transfer using REVERT Total Protein
231 Stain and Wash, as per manufacturer's instructions. Nitrocellulose membranes were blocked in
232 an appropriate buffer (Intercept® 1:1 PBS, 5% milk/PBS or 5% BSA/PBS) for 1 hour at room
233 temperature. Primary and secondary antibodies were diluted in blocking buffer 0.1% Tween-20,
234 with incubations overnight at 4°C or 1 hour at room temperature, respectively. Western blots
235 were imaged using the Odyssey CLx (LI-COR Biosciences, US) in 700nm and 800nm channels.
236 Quantification of protein signals was achieved using Image Studio Lite.
237

238 Primary antibodies: anti-SMN (BD Biosciences, 610646, 0.05 µg/ml), anti-ATM (Abcam,
239 ab32420, 0.12 µg/ml), anti-ATM phospho (Abcam, ab81292, 0.28 µg/ml), anti-alpha tubulin
240 (Abcam, ab4074, 0.33 µg/ml). Secondary antibodies: IRDye 800CW goat anti-mouse IgG
241 (LiCor, 926-32210, 0.5 µg/ml), goat anti-rabbit IgG Alexa Fluor 680 (Invitrogen, A-21076, 0.4
242 µg/ml).
243

244 Western blots were carried out on liver and spinal cord tissues from *Smn*$^{2B-/}$ mice, which were
245 extracted as previously described (37) using 2X modified RIPA buffer (2% NP-40, 0.5%
246 deoxycholic acid, 2 mM EDTA, 300 mM NaCl and 100 mM Tris-HCl (pH 7.4)). Firstly, the
247 tissues were diced and added to the extraction buffer and homogenized with pellet pestles,
248 then, after 5 minutes on ice, the tissues were sonicated at 5 microns for 10 s. This process was
249 repeated a further 2 times. The tissue extracts were centrifugated at 13,000 RPM (MSE,
250 Heathfield, UK; MSB010.CX2.5 Micro Centaur) for 5 minutes at 4°C and their protein
251 concentrations calculated using a BCA protein assay (PierceTM, 23227). Following adjustment
252 of protein levels, the tissue extracts were heated for 3 minutes at 95°C in 2X SDS sample buffer
253 (4% SDS, 10% 2-mercaptoethanol, 20% glycerol, 0.125 M Tris-HCl (pH 6.8) and bromophenol
254 blue) then loaded onto 4-12% Bis-Tris polyacrylamide gels for SDS-PAGE. The gel was excised
255 along the horizontal axis at a molecular weight greater than that expected for SMN (38 kDa) and
256 the proteins in the lower half of the gel were transferred onto a nitrocellulose membrane
257 overnight via western blot then blocked with 4% powdered milk in PBS. The membranes were
258 probed for SMN with the mouse anti-SMN antibody (MANSMA12 2E6 (38)), at either 1:50 or
259 1:100 for 2 hours and subsequently incubated with HRP-labelled rabbit anti-mouse Ig (DAKO,
260 P0260) at 0.25 ng/ml for 1h. Both incubations were at room temperature and antibodies
261 prepared in diluent (1% FBS, 1% horse serum (HS), 0.1% bovine serum albumin (BSA) in PBS
262 with 0.05% Triton X-100). Following incubation with West Pico, SMN-positive bands were
263 imaged with the Gel Image Documentation system (Bio-Rad). Total protein was assessed in the
264 upper half of the gel via Coomassie blue staining, and these data were used as the internal
265 loading control for each sample. ImageJ Fiji software (v1.51; (39)) was used to analyse both
266 antibody reactive and Coomassie-stained gel bands.
267

268 *Statistical analyses*

269 Data are presented as mean ± standard deviation. For all experiments where replicate data are
270 presented, at least n = 3 biological replicates were used, unless otherwise stated in specific
271 sections. A range of statistical tests were used, with the most appropriate test for each dataset
272 being determined individually. Data were tested for a normal distribution wherever possible, and
273 appropriate parametric and non-parametric tests were used accordingly.
274

275 Results

276

277 *Lentiviral and AAV9 vectors used for over-expression of* hSMN1

278 To test whether production of SMN could be improved by codon-optimisation of *hSMN1*, we
279 used a wild-type *hSMN1* cDNA and engineered an optimised form using a customised
280 commercial procedure. A comparison of wild-type and *Co-hSMN1* cDNAs is shown in Fig. S1.
281 Both cDNAs were cloned into several lentiviral plasmid backbones under the control of CMV,
282 hSYN and hPGK promoters and in all cases, followed by a mutated form of the WPRE
283 sequence (to prevent putative expression of woodchuck hepatitis virus X protein; Fig. 1A-C).
284 These transfer plasmids were used to produce integrating and integration-deficient lentiviral
285 vectors. Finally, the *Co-hSMN1* transgene was also cloned into an AAV plasmid backbone
286 under the control of the CAG promoter, followed by a mutated WPRE element (Fig. 1E). This
287 plasmid, as well as a control AAV_CAG_*eGFP* plasmid (Fig. 1F), was used to produce single-
288 stranded AAV9 vectors for *in vivo* use.
289

290 *Over-expression of codon-optimised* hSMN1 *in primary neuronal cultures*

291 Mouse cortical neuron cultures and rat motor neuron cultures were characterised as shown in
292 Fig. S2, demonstrating the expected morphology and the presence of relevant markers.

293 Integration-proficient (IPLV) and integration-deficient (IDLV) lentiviral vectors driven by the CMV
294 or hSYN promoters, encoding either wild-type *hSMN1* or the novel codon-optimised *Co-hSMN1*
295 transgene were used to transduce the cultures (Fig. 2). Dose-dependent increases in mean
296 SMN fluorescence intensity were seen by western blot in cortical neurons and
297 immunofluorescence in motor neurons (Fig. 2B,D and Tables S1,2). IPLV delivery led to higher
298 expression levels than with IDLVs, but SMN protein levels from the latter were also considerably
299 elevated. In terms of the promoter, CMV resulted in higher SMN levels regardless of vector
300 integration proficiency. The codon-optimised transgene led to significant increases in SMN
301 production in all cases, highlighting the improvements that this technology can afford for
302 transgenic gene expression.
303

304 *Characterisation of* Co-hSMN1 *IDLVs in human iPSC-derived MNs*

305 Three different wild-type and three SMA type I iPSC clones were differentiated into MNs with
306 high efficiency, exhibiting a characteristic neural network and individual cellular morphology
307 (Fig. 3A) with >90% OLIG2 positive MN progenitors at day 16 and 77.3% SMI-32-, 61.4% HB9-
308 and 90.1% ChAT-positive MNs at maturity (Fig. S3). A lack of full-length *SMN1* transcripts (Fig.
309 S4) and an 18-fold reduction in SMN protein (Fig. S4) were evident in SMA type I MNs
310 compared to wild-type cells ($P<0.0001$).
311

312 Transduction of SMA type I iPSC-derived MNs with IDLV_*Co-hSMN1* driven by CMV, hSYN or
313 PGK promoters led to an increase in SMN protein levels, detected by both immunofluorescence
314 (Fig. 3B) and western blot (Fig. 3C,D). Quantitation of western blot data showed that SMN
315 protein was increased in all transduced samples compared to untransduced counterparts (Fig.
316 3D). IDLVs expressing *Co-hSMN1* under the transcriptional control of either CMV or hPGK
317 promoters were able to significantly increase SMN protein production in all iPSC MN lines (Fig.

318 3D), whereas IDLV_hSYN_*Co-hSMN1* only led to a significant increase in CS13iSMAI-nxx.
319 Maximal SMN protein levels were observed with IDLVs expressing *Co-hSMN1* under the
320 transcriptional control of CMV (line SMA-19: 79.8-fold, P<0.0001; CS13iSMAI-nxx: 14.5-fold,
321 P<0.0001; CS32iSMAI-nxx: 42.8-fold, P<0.0001). When levels were compared to those in wild-
322 type iPSC MNs, supraphysiological SMN protein was evident in SMA-19 and CS32iSMAI-nxx
323 lines, but not in CS13iSMAI-nxx.
324

325 *Transduction and rescue of human SMA type I fibroblasts by lentiviral vectors encoding* Co-
326 hSMN1

327 Cultured human wild-type or type I SMA fibroblasts were transduced with IDLVs encoding wild-
328 type or *Co-hSMN1* under CMV, hSYN or hPGK promoters. A clear increase in cytoplasmic SMN
329 was seen by immunofluorescence in both wild-type and SMA type I fibroblasts following IDLV
330 transduction (Fig. 4A) and a statistically significant increase was confirmed by western blot (Fig.
331 4B,C). Analysis of total SMN levels in transduced fibroblasts (Fig. 4C) corroborated the pattern
332 of expression seen in SMA type I iPSC-MNs (Fig. 3D), where CMV-driven vectors were able to
333 increase SMN expression to the highest extent, followed by hPGK and then hSYN-driven
334 vectors.
335

336 SMA type I fibroblasts were transduced with IPLVs and IDLVs to determine the effectiveness of
337 each vector to restore SMN-expressing nuclear gems, which are largely absent in SMA type I
338 samples. All vectors were able to restore the presence of gems in transduced cells (Fig. 5A and
339 Table S3) in an MOI-dependent manner (Fig. 5B). At the highest MOI tested (MOI 100), no
340 visible changes in cell morphology were seen, suggesting absence of vector-mediated toxicity.
341 IPLV transduction led to a 1.6-fold greater number of gems than in IDLV-transduced cells
342 (P=0.0015), regardless of promoter or transgene (Fig. 5B). Moreover, *Co-hSMN1* led to the

343 restoration of a significantly higher number of gems than wild-type *hSMN1* (1.7-fold, P=0.0005).
344 With regards to choosing the optimal promoter, CMV-driven vectors were able to increase gem
345 number by 1.8-fold compared to hSYN-driven vectors (P= 0.0003). In some cases, a higher
346 number of gems was seen in transduced SMA type I fibroblasts than in healthy cells.
347

348 *Analysis of downstream DNA damage markers following* in vitro *IDLV transduction*

349 The molecular links between SMN and DNA damage- and apoptosis-related proteins (40-43)
350 are not completely clear but learning how SMN interacts with these pathways may be important
351 in understanding why SMA MNs degenerate and how this could be modulated by treatment with
352 an *SMN*-encoding vector. It is also important to understand the consequences of SMN
353 restoration to wild-type or supraphysiological levels, and what effect this might have on cells that
354 have always been severely deficient in SMN.
355

356 γH2AX foci are hallmarks of DNA damage (44, 45) and immunofluorescent detection of these in
357 untreated wild-type and SMA type I fibroblasts revealed distinct foci in nuclei of both genotypes,
358 but these were seen more frequently in SMA type I cells (Fig. 6A). Both the number of foci per
359 cell and the percentage of cells exhibiting any number of foci were significantly higher in SMA
360 type I samples (Fig. 6B,C; P=0.0057 and P=0.0069, respectively). Upon transduction of SMA
361 type I fibroblasts with IDLV_CMV_*Co-hSMN1* (the IDLV vector shown to be most potent in
362 previous experiments), signs of DNA damage were increased further as the number of γH2AX
363 foci, and γH2AX foci-positive cells increased significantly, compared to mock-treated SMA type I
364 cells (Fig. 6B,C; P=0.0134 and P=0.0068, respectively). At this stage, it is unclear whether this
365 increase was due to the act of lentiviral transduction, or due to a sudden increase in SMN levels
366 in cells that had always been deficient. Of note, no increase in levels of cleaved caspase 3, a

367 marker of DNA damage and apoptosis (46), was observed in IDLV_*Co-hSMN1*-transduced
368 SMA type I fibroblasts (Fig. S5).
369
370 ATM, specifically its phosphorylated form, acts as a chief mobiliser of cellular DNA damage and
371 apoptotic pathways that may be active in SMA cells (47). Levels of total ATM were found to be
372 equal in both wild-type and SMA type I fibroblasts according to quantitated western blots (Fig.
373 7A; P=0.6662 and Fig. S6), with the phosphorylated form only showing a trend for increased
374 signal in the mutant cells (Fig. 7B; P>0.05). Phosphorylated ATM could be significantly
375 increased by treatment of the cells with 200 μM hydrogen peroxide for 2 hours (Fig. 7B; wild-
376 type vs SMA+H_2O_2 P<0.01, SMA vs SMA+H_2O_2 P<0.05). Following transduction of SMA type I
377 fibroblasts with either IDLV_CMV_*eGFP* or IDLV_CMV_*Co-hSMN1*, phosphorylated ATM was
378 assessed. At 3 days post-transduction, pATM was significantly increased in IDLV_CMV_*eGFP*
379 treated cells, but not in IDLV_CMV_*Co-hSMN1* (Fig. 7C; P=0.0160 and P=0.4983, respectively).
380 pATM remained relatively high in IDLV_CMV_*eGFP* treated cells at 7 days post-transduction
381 (Fig. 7C; P=0.0002), whereas in IDLV_CMV_*Co-hSMN1*-transduced cells dropped below that of
382 mock samples (Fig. 7C; P=0.0256). ATM and pATM levels were also measured in SMA type I
383 iPSC-derived MNs, mock-transduced or treated with IDLV_CMV_*Co-hSMN1*. No effect of
384 transduction on total ATM was observed, but a significant increase in pATM was seen in two out
385 of three SMA type I iPSC-MN lines at 3 days post-transduction (Fig. 7D,E; SMA-19 P<0.0001,
386 CS13iSMAI-nxx P=0.0003, CS32iSMAI-nxx P=0.0160).
387
388 Together, these data show that at least two markers of DNA damage are increased in the short-
389 term window following lentiviral transduction of SMA cells. As pATM levels then normalised
390 again, and were even reduced to below those of untreated cells, we suggest that this short-term
391 increase in DNA damage markers is due to the act of transduction, rather than our *Co-hSMN1*

392 transgene. Although γH2AX foci were not measured at later time points, we suspect this
393 outcome measure would follow the same pattern.
394

395 In vivo *expression from AAV_CAG_*Co-hSMN1 *in the* Smn$^{2B/-}$ *mouse model of SMA*

396 To test the expression of *Co-hSMN1 in vivo*, we chose the *Smn$^{2B/-}$* mouse model of SMA, where
397 over-expression of the transgene would be easily detected above low background levels of the
398 protein. An AAV9 vector driven by the CAG promoter and including a mutated WPRE element
399 was produced, and an AAV9_CAG_*eGFP* vector used as a control. These vectors were
400 delivered to neonatal mice and SMN expression assessed in liver and spinal cord samples
401 harvested at the symptomatic time-point of P18.
402

403 Livers of untreated and AAV9_CAG_*eGFP*-treated *Smn$^{2B/-}$* mice showed significantly less SMN
404 than wild-type controls (Fig. 8A,B; P=0.0377 and P=0.0118, respectively), whereas those
405 treated with AAV9_CAG_*Co-hSMN1* exhibited 1.7-fold of wild-type levels (Fig. 8A,B; SMN vs
406 wild-type P=0.0725, SMN vs *Smn$^{2B/-}$* P=0.0005). Data from spinal cord samples showed
407 similarly low levels of SMN in *Smn$^{2B/-}$* mice, and more variability in AAV9_CAG_*Co-hSMN1*
408 treated mice, but a 2.6-fold increase above wild-type SMN levels was still seen (Fig. 8C,D; SMN
409 vs wild-type P=0.5260, SMN vs *Smn$^{2B/-}$* P=0.0162).
410

411 Discussion

412 Gene therapy allows the modification of gene expression for therapeutic purposes, whereby
413 gene addition involves the introduction of a functional transgene into the appropriate cells of the
414 host. Therefore, the efficient delivery of therapeutic genes and appropriate gene expression
415 systems are critical requirements for the development of an effective treatment (48). Benefits of

416 an optimised system include significant reduction of vector dose needed to maintain transgene
417 expression and lead to sufficient levels of protein production. Therefore, this study aimed to
418 optimise a novel expression cassette for SMA, assessing integrative ability, promoters and
419 transgene sequences for their effect on vector expression.
420
421 Our *in vitro* SMN restoration data provides similar results to those reported for existing lentiviral
422 (49) and adenoviral (50) transduction as well as plasmid lipofection (51) and gene targeting
423 (52). Limited use of lentiviral vectors for *in vivo* treatment of SMA has been reported, with the
424 early exception of Azzouz and colleagues (53). Here, we show evidence that a lentiviral
425 expression system can efficiently restore SMN protein levels, especially when expressing our
426 optimised transgene, *Co-hSMN1*. The four seminal papers that first demonstrated that viral
427 vector-mediated expression of *SMN1 in vivo* on the day of birth provides amelioration of SMA
428 phenotype, all used AAV vectors (54-57). Whilst these provided invaluable data and later led to
429 the approval of Zolgensma as a licensed SMA therapy, it is also clear that no curative treatment
430 is yet available for SMA. Our goal has been to develop a novel expression cassette,
431 implemented in lentiviral vectors for cell culture testing and localised delivery *in vivo*, and in AAV
432 vectors for widespread *in vivo* distribution.
433
434 Our optimisation has revealed that both IPLV and IDLV configurations encoding *SMN1* variants
435 are efficient at transducing various *in vitro* models. Generally, IPLVs resulted in higher
436 expression levels compared to their IDLV counterparts, although significant expression could
437 still be obtained with the latter. The expression levels mediated by the IDLVs may actually be
438 more adequate, as it has come to light that supraphysiological levels of SMN may be toxic (58),
439 and IDLVs are a safer option without the potential risk of insertional mutagenesis from IPLVs.
440 Transgenic expression levels of *SMN1* can also be controlled through the choice of promoter.
441 Our *in vitro* experiments revealed that the ubiquitous CMV promoter directed the most robust

442 transgene expression from lentiviral vectors. The strong and constitutive nature of this promoter
443 lends itself to the systemic nature of SMA, as CMV can mediate gene expression in a
444 remarkably broad range of cells. Intermediate transgenic expression levels were achieved with
445 the ubiquitous hPGK promoter, while the neuron-specific hSYN promoter appeared the weakest
446 of the three, despite the use of relevant neuronal systems as well as human fibroblasts.
447
448 Codon-optimisation of the *hSMN1* cDNA had a significant positive impact on the efficiency of
449 the transgenic expression in all the cell culture systems evaluated. Implementation of the
450 optimised transgene in an AAV9 vector for *in vivo* delivery in *Smn*$^{2B/-}$ mice demonstrated robust
451 expression in liver and spinal cord, at somewhat variable levels that on average were not
452 significantly different from wild-type. Whilst the scope of the *in vivo* work presented here was
453 limited to demonstrating effective transgenic expression, our cell culture experiments have
454 shown dose-dependent expression from lentiviral vectors, which presumably could be replicated
455 *in vivo* to titrate expression levels to an optimum. This is important, given the potential toxicity of
456 SMN over-production (58).
457
458 The goal of maximizing correction of the SMA phenotype through the concurrent actions of
459 several therapeutic compounds, or delivery routes, is gaining traction within the SMA field (59).
460 Combinatorial delivery of a systemic AAV9 and a locally injected AAV or lentiviral vector to
461 reinforce strong expression at specific locations might be a future avenue of investigation. A
462 second possible strategy in which to use either AAV or lentiviral vectors expressing *SMN* would
463 be *in utero* delivery. This has been attempted recently for SMA using AAV9 vectors and
464 intracerebroventricular injections in mice fetuses. The results have shown encouraging rescue
465 of the SMA phenotype but also significantly enhanced abortion rates of SMA mice compared to
466 heterozygous or wild-type counterparts, pointing to potentially increased sensitivity to the
467 procedure in SMA animals (60). Fetal delivery of IDLVs injected intraspinally has led to

468 widespread expression of *eGFP* at all levels of the spinal cord in mice, underscoring the
469 potential promise of this delivery system (61).
470
471 Several groups have found proteins associated with DNA damage and apoptosis to be
472 dysregulated in SMA systems, including cleaved caspase 3 (41, 62), pATM , DNA-PKcs (43),
473 senataxin (43), CHK2, pBRCA1, p53 (63) and γH2AX (63, 64). Signals indicative of genomic
474 instability caused by DNA double strand breaks are transduced by ATM and downstream
475 proteins including H2AX, leading to DNA repair by proteins such as BRCA1; or if damage is too
476 severe, apoptosis. Evidence of SMN restoration being able to revert some molecular signatures
477 of the DNA damage response has been reported in the literature (40-43). In contrast, we found
478 here that lentiviral transduction caused an increase in pATM levels, in the percentage of SMA
479 fibroblasts that exhibited γH2AX foci as well as in the number of foci per cell, indicative of
480 activation of the DNA damage response pathway. However, we did observe that the *Co-hSMN1*
481 transgene had a protective effect in fibroblasts compared to *eGFP*-expressing vector regarding
482 the induction of pATM.
483
484 A possible explanation for increase in γH2AX foci and pATM following IDLV transduction could
485 be short-term initiation of host anti-viral responses which then activate the DNA damage
486 response pathway. Lentiviral vector transduction is likely to trigger host anti-viral responses
487 causing an increase in Toll-like receptor- (65) and type I interferon-signaling (66). Endocytosis
488 of vectors, presence of the RNA:DNA hybrids following reverse transcription acting as a
489 pathogen-associated molecular pattern, or plasmid contamination in laboratory-grade vector
490 preparations could all alert the cell to presence of the viral vector (65). Finally, third generation
491 lentiviral vectors lack pathogenic proteins such as Vpr, whose role normally is to counteract host
492 anti-viral factors (65). Interferon-γ treatment has been shown to activate ATM (67), a process

493 that involves autophosphorylation thus leading to increased pATM, like that seen here in SMA
494 type I cells. Unrepaired DNA lesions, such as those evidenced by the increased γH2AX foci in
495 SMA fibroblasts seen here, prime the type I interferon system leading to enhanced anti-viral
496 responses upon encounter with viral particles (67, 68), potentially explaining why lentiviral
497 vector transduction increased levels of γH2AX protein further. Following on from our work,
498 further investigations are needed into both the benefits and potential detriments of viral
499 transduction, specifically with regard to DNA damage and apoptotic protein expression changes
500 following *in vivo* administration.
501
502 The outlook of therapy for SMA is continuing to look positive with three therapies licensed for
503 clinical use, as well as an increasing number of other therapeutic strategies in the pipeline.
504 Here, we have presented promising steps towards the development of a new strategy focused
505 on delivery of a codon-optimised transgene, *Co-hSMN1*. Lentiviral-mediated expression of *Co-*
506 *hSMN1* is able to rescue SMN expression in multiple *in vitro* cell systems and AAV9 delivery
507 leads to strong expression in the $Smn^{2B/-}$ mouse model of SMA. Future experimentation should
508 continue to explore long-term benefits of this therapeutic strategy on survival and motor
509 performance of SMA mice, whilst also delving into any unexpected genotoxic consequences of
510 viral transduction.
511

512 Author contributions

513 EMC and NAMN performed *in vitro* experimentation and analyses. MB performed *in vivo*
514 injections and tissue harvests whilst SO analysed tissue from *in vivo* experiments. HF provided
515 support for animal experimentation. RJY-M provided conceptual support and interpretation of
516 results. All authors contributed to manuscript preparation.

Competing interests

NAMN, EMC and RJY-M have filed a patent application on the uses of the novel SMN transgene reported in this manuscript. SB, HRF and MB report no conflicts of interest.

Funding

EMC was partially funded by a scholarship from Royal Holloway University of London. NAMN was partially funded by a scholarship and student stipend, from Royal Holloway University of London and The Spinal Muscular Atrophy Trust. HF acknowledges financial support for SMA research from the Great Ormond Street Hospital Charity (GOSH) which funds SO (Grant No. V5018). RJY-M acknowledges general financial support from SMA UK (formerly The SMA Trust), through the UK SMA Research Consortium, for SMA research in his laboratory. MB acknowledges general financial support from SMA UK, Muscular Dystrophy UK, Action Medical Research, SMA Angels Charity and Academy of Medical Sciences for SMA research in her laboratory.

References

1. Lefebvre S, Burgen L, Reboullet S, Clermont O, Burlet P, Viollet L, et al. Identification and characterisation of a spinal muscular atrophy-determining gene. Cell. 1995;80(155-165).
2. Lorson CL, Hahnen E, Androphy EJ, Wirth B. A single nucleotide in the SMN gene regulates splicing and is responsible for spinal muscular atrophy. Proc Natl Acad Sci U S A. 1999;96(11):6307-11.
3. Monani UR, Lorson CL, Parsons DW, Prior TW, Androphy EJ, Burghes AHM, et al. A single nucleotide difference that alters splicing patterns distinguishes the SMA gene SMN1 from the copy gene SMN2. Human Molecular Genetics. 1999;8(7):1177-83.
4. Butchbach MER. Copy Number Variations in the Survival Motor Neuron Genes: Implications for Spinal Muscular Atrophy and Other Neurodegenerative Diseases. Frontiers in Molecular Biosciences. 2016;3.
5. Harada Y, Sutomo R, Sadewa A, Akutsu T, Takeshima Y, Wada H, et al. Correlation between SMN2 copy number and clinical phenotype of spinal muscular atrophy: three SMN2 copies fail to rescue some patients from the disease severity. J Neurol. 2002;249:1211-9.
6. Calucho M BS, Alías L, March F, Venceslá A, Rodríguez-Álvarez FJ, Aller E, Fernández RM, Borrego S, Millán JM, Hernández-Chico C, Cuscó I, Fuentes-Prior P, Tizzano EF. .

550 Correlation between SMA type and SMN2 copy number revisited: An analysis of 625 unrelated
551 Spanish patients and a compilation of 2834 reported cases. . Neuromuscul Disord
552 2018;28(3):208-15.
553 7. Singh RN, Howell MD, Ottesen EW, Singh NN. Diverse role of survival motor neuron
554 protein. Biochemica et Biophysica Acta. 2017;1860:299-315.
555 8. Gavrilina TO, McGovern VL, Workman E, Crawford TO, Gogliotti RG, DiDonato CJ, et
556 al. Neuronal SMN expression corrects spinal muscular atrophy in severe SMA mice while
557 muscle-specific SMN expression has no phenotypic effect. Human Molecular Genetics.
558 2008;17:1063-75.
559 9. Hamilton G, Gillingwater TH. Spinal muscular atrophy: going beyond the motor neuron.
560 Trends in Molecular Medicine. 2013;19(1):40-50.
561 10. Singh NK, Singh NN, Androphy EJ, Singh RN. Splicing of a critical exon of human
562 survival motor neuron is regulated by a unique silencer element located in the last intron.
563 Molecular and Cellular Biology. 2006;26(4):1333-46.
564 11. Singh NN, Howell MD, Androphy EJ, Singh RN. How the discovery of ISS-N1 led to the
565 first medical therapy for spinal muscular atrophy. Gene Therapy. 2017;24(9):520-6.
566 12. Mendell JR, Al-Zaidy S, Shell R, Arnold WD, Rodino-Klapac LR, Prior TW, et al. Single-
567 Dose Gene-Replacement Therapy for Spinal Muscular Atrophy. New England Journal of
568 Medicine. 2017;377(18):1713-22.
569 13. Baranello G, Darras BT, Day JW, Deconinck N, Klein A, Masson R, et al. Risdiplam in
570 Type 1 Spinal Muscular Atrophy. New England Journal of Medicine. 2021;384(10):915-23.
571 14. Blömer U, Naldini L, Kafri T, Trono D, Verma IM, Gage FH. Highly efficient and
572 sustained gene transfer in adult neurons with a lentivirus vector. . Journal of Virology.
573 1997;71:6641–9.
574 15. Frankel D, Young J. HIV-1: fifteen proteins and an RNA. . Annual Review of
575 Biochemistry. 1998;67:1–25.
576 16. Picanco-Castro V, de Sousa Russo-Carbolante EM, Tadeu Covas D. Advances in
577 lentiviral vectors: a patent review. Recent Patents on DNA & Gene Sequences. 2012;6:82–90.
578 17. Vigna E, Naldini L. Lentiviral vectors: excellent tools for experimental gene transfer and
579 promising candidates for gene therapy. Journal of Gene Medicine. 2000;2(5):308-16.
580 18. Throm RE, Ouma AA, Zhou S, Chandrasekaran A, Lockey T, Greene M, et al. Efficient
581 construction of producer cell lines for a SIN lentiviral vector for SCID-X1 gene therapy by
582 concatemeric array transfection. Blood. 2009;113:5104–10.
583 19. Zhao H, Pestina TI, Nasimuzzaman M, Mehta P, Hargrove PW, Persons DA.
584 Amelioration of murine beta-thalassemia through drug selection of hematopoietic stem cells
585 transduced with a lentiviral vector encoding both gamma-globin and the MGMT drug-resistance
586 gene. Blood. 2009;113:5747–56.
587 20. Mantovani J, Charrier S, Eckenberg R, Saurin W, Danos O, Perea J, et al. Diverse
588 genomic integration of a lentiviral vector developed for the treatment of Wiskott-Aldrich
589 syndrome. The Journal of Gene Medicine. 2009;11:645–
590 54.
591 21. Biffi A, Naldini L. Novel candidate disease for gene therapy: metachromatic
592 leukodystrophy. Expert Opinion on Biological Therapy. 2007;7:1193– 205.
593 22. Brown BD, Cantore A, Annoni A, Sergi LS, Lombardo A, Della Valle P, et al. A
594 microRNA-regulated lentiviral vector mediates stable correction of hemophilia B mice. Blood.
595 2007;110:4144–52.
596 23. Jacome A, Navarro S, Río P, Yañez RM, González-Murillo A, Lozano ML, et al.
597 Lentiviral-mediated genetic correction of hematopoietic and mesenchymal progenitor cells from
598 Fanconi anemia patients. . Molecular Therapy. 2009;17:1083–92.

599 24. Menzel O, Birraux J, Wildhaber BE, Jond C, Lasne F, Habre W, et al. Biosafety in ex
600 vivo gene therapy and conditional ablation of lentivirally transduced hepatocytes in nonhuman
601 primates. Molecular Therapy. 2009;17:1754–60.
602 25. Schuster SJ, Bishop, M. R., Tam, C. S., Waller, E. K., Borchmann, P., Mcguirk, J. P., et
603 al. Primary analysis of juliet: a global, pivotal, phase 2 Trial of CTL019 in adult patients with
604 relapsed or refractory diffuse large B-cell lymphoma. . Blood. 2017;130:577-.
605 26. Maude SL, Laetsch, T. W., Buechner, J., Rives, S., Boyer, M., Bittencourt, H., et al.
606 Tisagenlecleucel in Children and Young Adults with B-Cell Lymphoblastic Leukemia. . New
607 England Journal of Medicine. 2018;378:439–48.
608 27. Thompson AA, Walters MC, Kwiatkowski J, Rasko JEJ, Ribeil J-A, Hongeng S, et al.
609 Gene Therapy in Patients with Transfusion-Dependent β-Thalassemia. New England Journal of
610 Medicine. 2018;378(16):1479-93.
611 28. Hacein-Bey-Abina S, Von Kalle C, Schmidt M, McCcormack MP, Wulffraat N, Leboulch
612 P, et al. LMO2-associated clonal T cell proliferation in two patients after gene therapy for SCID-
613 X1. Science. 2003;302(5644):415-9.
614 29. Gaspar HB, Parsley KL, Howe S, King D, Gilmour KC, Sinclair J, et al. Gene therapy of
615 X-linked severe combined immunodeficiency by use of a pseudotyped gammaretroviral vector.
616 Lancet. 2004;364(9452):2181-7.
617 30. Howe SJ, Mansour MR, Schwarzwaelder K, Bartholomae C, Hubank M, Kempski H, et
618 al. Insertional mutagenesis combined with acquired somatic mutations causes leukemogenesis
619 following gene therapy of SCID-X1 patients. Journal of Clinical Investigation. 2008;118(9):3143-
620 50.
621 31. Yáñez-Muñoz RJ, Balaggan KS, MacNeil A, Howe SJ, Schmidt M, Smith AJ, et al.
622 Effective gene therapy with nonintegrating lentiviral vectors. Nature Medicine. 2006;12(3):348-
623 53.
624 32. Bowerman M, Murray LM, Beauvais A, Pinheiro B, Kothary R. A critical smn threshold in
625 mice dictates onset of an intermediate spinal muscular atrophy phenotype associated with a
626 distinct neuromuscular junction pathology. Neuromuscular Disorders. 2012;22(3):263-76.
627 33. Boza-Moran MG, Martinez-Hernandez R, Bernal S, Wanisch K, Also-Rallo E, Le Heron
628 A, et al. Decay in survival motor neuron and plastin 3 levels during differentiation of iPSC-
629 derived human motor neurons. Scientific Reports. 2015;5:11696.
630 34. Lu-Nguyen NB, Broadstock M, Yáñez-Muñoz RJ. Efficient expression of Igf-1 from
631 lentiviral vectors protects in vitro but does not mediate behavioral recovery of a Parkinsonian
632 lesion in rats. Human Gene Therapy. 2015;26:719-33.
633 35. Peluffo H, Foster E, Ahmed SG, Lago N, Hutson TH, Moon L, et al. Efficient gene
634 expression from integration-deficient lentiviral vectors in the spinal cord. Gene Ther.
635 2013;20(6):645-57.
636 36. Maury Y, Come J, Piskorowski RA, Salah-Mohellibi N, Chevaleyre V, Peschanski M, et
637 al. Combinatorial analysis of developmental cues efficiently converts human pluripotent stem
638 cells into multiple neuronal subtypes. Nature Biotechnol. 2015;33(1):89-96.
639 37. Šoltić D, Bowerman M, Stock J, Shorrock HK, Gillingwater TH, H.R. F. Multi-Study
640 Proteomic and Bioinformatic Identification of Molecular Overlap between Amyotrophic Lateral
641 Sclerosis (ALS) and Spinal Muscular Atrophy (SMA). Brain Sciences. 2018;8(212).
642 38. Young PJ, Le TT, Thi Man N, Burghes AHM, Morris GE. The relationship between SMN,
643 the spinal muscular atrophy protein, and nuclear coiled bodies in differentiated tissues and
644 cultured cells. Exp Cell Res. 2000;256:365-74.
645 39. Abràmoff MD, Magalhães PJ, Ram SJ. Image processing with imageJ. . Biophotonics
646 Int. 2004;11:36-41.
647 40. Vyas S, Bechade C, Riveau B, Downward J, Triller A. Involvement of survival motor
648 neuron (SMN) protein in cell death. Human Molecular Genetics. 2002;11(22):2751-64.

649 41. Parker GC, Li XL, Anguelov RA, Toth G, Cristescu A, Acsadi G. Survival motor neuron
650 protein regulates apoptosis in an in vitro model of spinal muscular atrophy. Neurotoxicity
651 Research. 2008;13(1):39-48.
652 42. Young PJ, Day PM, Zhou J, Androphy EJ, Morris GE, Lorson CL. A direct interaction
653 between the survival motor neuron protein and p53 and its relationship to spinal muscular
654 atrophy. Journal of Biological Chemistry. 2002;277(4):2852-9.
655 43. Kannan A, Bhatia K, Branzei D, Gangwani L. Combined deficiency of Senataxin and
656 DNA-PKcs causes DNA damage accumulation and neurodegeneration in spinal muscular
657 atrophy. Nucleic Acids Research. 2018;46(16):8326-46.
658 44. Rogakou EP, Pilch DR, Orr AH, Ivanova VS, Bonner WM. DNA double-stranded breaks
659 induce histone H2AX phosphorylation on serine 139. Journal of Biological Chemistry.
660 1998;273(10):5858-68.
661 45. Rogakou EP, Boon C, Redon C, Bonner WM. Megabase chromatin domains involved in
662 DNA double-strand breaks in vivo. Journal of Cell Biology. 1999;146(5):905-15.
663 46. Martin SJ, Green DR. Protease activation during apoptosis: death by a thousand cuts?
664 Cell. 1995;82(3):349-52.
665 47. Blackford AN, Jackson SP. ATM, ATR, and DNA-PK: The Trinity at the Heart of the DNA
666 Damage Response. Mol Cell. 2017;66(6):801-17.
667 48. Walther W, Stein U. Viral vectors for gene transfer: a review of their use in the treatment
668 of human diseases. Drugs. 2000;60:249–71.
669 49. Valori CF, Ning K, Wyles M, Mead RJ, Grierson AJ, Shaw PJ, et al. Systemic delivery of
670 scAAV9 expressing SMN prolongs survival in a model of spinal muscular atrophy. Science
671 Translational Medicine. 2010;2(35):35ra42.
672 50. DiDonato CJ, Parks RJ, Kothary R. Development of a gene therapy strategy for the
673 restoration of survival motor neuron protein expression: implications for spinal muscular atrophy
674 therapy. Human Gene Therapy. 2003;14(2):179-88.
675 51. Rashnonejad A, Chermahini GA, Li SY, Ozkinay F, Gao GP. Large-Scale Production of
676 Adeno-Associated Viral Vector Serotype-9 Carrying the Human Survival Motor Neuron Gene.
677 Molecular Biotechnology. 2016;58(1):30-6.
678 52. Feng M, Liu C, Xia Y, Liu B, Zhou M, Li Z, et al. Restoration of SMN expression in
679 mesenchymal stem cells derived from gene-targeted patient-specific iPSCs. Journal of
680 Molecular Histology. 2018;49:27-37.
681 53. Azzouz M, Le T, Ralph GS, Walmsley L, Monani UR, Lee DC, et al. Lentivector-
682 mediated SMN replacement in a mouse model of spinal muscular atrophy. Journal of Clinical
683 Investigation. 2004;114(12):1726-31.
684 54. Foust KD, Wang XY, McGovern VL, Braun L, Bevan AK, Haidet AM, et al. Rescue of the
685 spinal muscular atrophy phenotype in a mouse model by early postnatal delivery of SMN.
686 Nature Biotechnology. 2010;28(3):271-U126.
687 55. Passini MA, Bu J, Roskelley EM, Richards AM, Sardi SP, O'Riordan CR, et al. CNS-
688 targeted gene therapy improves survival and motor function in a mouse model of spinal
689 muscular atrophy. J Clin Invest. 2010;120(4):1253-64.
690 56. Valori CF, Ning K, Wyles M, Mead RJ, Grierson AJ, Shaw PJ, et al. Systemic delivery of
691 scAAV9 expressing SMN prolongs survival in a model of spinal muscular atrophy. Sci Transl
692 Med. 2010;2(35):35ra42.
693 57. Dominguez E, Marais T, Chatauret N, Benkhelifa-Ziyyat S, Duque S, Ravassard P, et al.
694 Intravenous scAAV9 delivery of a codon-optimized SMN1 sequence rescues SMA mice. Hum
695 Mol Genet. 2011;20(4):681-93.
696 58. Van Alstyne M, Tattoli I, Delestree N, Recinos Y, Workman E, Shihabuddin LS, et al.
697 Gain of toxic function by long-term AAV9-mediated SMN overexpression in the sensorimotor
698 circuit. Nature Neuroscience. 2021;24(7):930-+.

59. Bowerman M, Becker CG, Yáñez-Muñoz RJ, Ning K, Wood M, Gillingwater TH, et al. Therapeutic strategies for spinal muscular atrophy: SMN and beyond. Disease Models & Mechanisms. 2017;10:943-54.
60. Rashnonejad A, Chermahini GA, Gunduz C, Onay H, Aykut A, Durmaz B, et al. Fetal Gene Therapy Using a Single Injection of Recombinant AAV9 Rescued SMA Phenotype in Mice. Molecular Therapy. 2019;27(12):2123-33.
61. Ahmed SG, Waddington SN, Boza-Moran MG, Yáñez-Muñoz RJ. High-efficiency transduction of spinal cord motor neurons by intrauterine delivery of integration-deficient lentiviral vectors. Journal of Controlled Release. 2018;273:99-107.
62. Sareen D, Ebert AD, Heins BM, Mcgivern JV, Ornelas L, Svendsen CN. Inhibition of Apoptosis Blocks Human Motor Neuron Cell Death in a Stem Cell Model of Spinal Muscular Atrophy. . Plos One. 2012;7.
63. Jangi M, Fleet C, Cullen P, Gupta SV, Mekhoubad S, Chiao E, et al. SMN deficiency in severe models of spinal muscular atrophy causes widespread intron retention and DNA damage. Proc Natl Acad Sci U S A. 2017;114(12):E2347-E56.
64. Mutsaers CA, Wishart, T.M., Lamont, D.J., Riessland, M., Schreml, J., Comley, L.H., Murray, L.M., Parson, S.H., Lochmuller, H., Wirth, B., Talbot, K., Gillingwater, T.H. . Reversible molecular pathology of skeletal muscle in spinal muscular atrophy. . Human Molecular Genetics. 2011;20:4334-44.
65. Kajaste-Rudnitski A, Naldini L. Cellular Innate Immunity and Restriction of Viral Infection: Implications for Lentiviral Gene Therapy in Human Hematopoietic Cells. Human Gene Therapy. 2015;26(4):201-9.
66. Maillard PV, van der Veen AG, Poirier EZ, Reis e Sousa C. Slicing and dicing viruses: antiviral RNA interference in mammals. Embo Journal. 2019;38(8).
67. Morales AJ, Carrero JA, Hung PJ, Tubbs AT, Andrews JM, Edelson BT, et al. A type I IFN-dependent DNA damage response regulates the genetic program and inflammasome activation in macrophages. Elife. 2017;6.
68. Hartlova A, Erttmann SF, Raffi FAM, Schmalz AM, Resch U, Anugula S, et al. DNA Damage Primes the Type I Interferon System via the Cytosolic DNA Sensor STING to Promote Anti-Microbial Innate Immunity. Immunity. 2015;42(2):332-43.

Figure legends

Figure 1: Maps displaying features of the transfer plasmids encoding *Co-hSMN1* or control *eGFP*.

The constructs used in transfer plasmids to produce (A-D) lentiviral or (E,F) adeno-associated viral (AAV) vectors are shown. Each plasmid encodes the *Co-hSMN1* or *eGFP* transgene flanked upstream by a promoter (CMV, hSYN, hPGK or chicken beta-actin CMV hybrid (CAG)) and downstream by woodchuck hepatitis post-transcriptional regulatory element (WPRE;

mutated in constructs A-C and E), a post-transcriptional element that improves transgene expression (except in the case of AAV_CAG_*eGFP* (F)).

Figure 2: Lentiviral vector-mediated *hSMN1* and *Co-hSMN1* expression in mouse primary cortical neurons and rat primary motor neurons.
3-week old mouse primary cortical cultures and isolated motor neuron cultures from E15 rat embryos were transduced with IPLVs and IDLVs encoding CMV_*hSMN1,* CMV_*Co-hSMN1,* hSYN_*hSMN1* or hSYN_*Co-hSMN1* cassettes, with cells collected at 72h post-transduction. (A) qPCR MOI 30 and 100 were used to transduce mouse cortical neuronal cultures, which were analysed by western blot and SMN protein levels were quantified in (B). Representative western blots are shown and statistical comparisons can be found in Table S1. (C) Motor neurons were transduced at qPCR MOI 30, 60 or 100. Immunofluorescence images show examples of transduced cells at MOI 60, 72h post-transduction. Scale bars = 20 µm. (D) Quantification of SMN immunofluorescence in cell bodies of transduced or control E14 rat primary motor neurons. Statistical comparisons can be found in Table S2. Error bars represent standard deviation. N=3 biological replicates were collected in each case.

Figure 3: Assessment of SMN protein levels in iPSC motor neurons. (A) Representative images of mature, SMA type I iPSC-derived motor neurons at both high and low seeding density. Scale bar = 100 µm (high density, top image) and 50 µm (low density, bottom image). (B) Immunofluorescence images of control and IDLV_CMV_*Co-hSMN1*-transduced SMA type I iPSC motor neurons. Scale bar = 20 µm (top image) and 50 µm (bottom image). (C) Representative western blots showing total protein (red) and SMN (green) in triplicate samples from three independent SMA type I iPSC MN lines mock-transduced or transduced with IDLVs expressing *Co-hSMN1* under transcriptional control of CMV, hSYN or hPGK promoters. (D) Quantification of western blots. Error bars represent standard deviation. No significant

difference was seen between the three untransduced wild type lines, or between the three SMA type I lines. Significance represented by stars on transduced samples indicates a comparison to the control SMN levels in that particular line. * P<0.05, ** P<0.01, *** P<0.001, **** P<0.0001. N=3 biological replicates were collected for each line, as well as three independent lines for each genotype used.

Figure 4: SMN levels in primary SMA type I patient fibroblasts following IDLV transduction.

(A) Representative immunofluorescent images of wild-type and SMA type I fibroblasts after IDLV_CMV_*Co-hSMN1* transduction at qPCR MOI 75 and 100, plus control. Scale bars = 50 µm in all images. (B) Western blots from cells harvested 72h post-transduction with IDLVs at MOI 75 and 100. (C) Quantification of western blots. Error bars represent standard deviation. * P<0.05, ** P<0.01, *** P<0.001, **** P<0.0001. N=3 biological replicates were collected in each case.

Figure 5: Restoration of gems in SMA type I fibroblasts transduced with lentiviral vectors encoding *hSMN1* or *Co-hSMN1*.

Cultured human SMA type I fibroblasts were transduced with IPLVs or IDLVs encoding CMV_*hSMN1,* CMV_*Co-hSMN1,* hSYN_*hSMN1* or hSYN_*Co-hSMN1* cassettes at qPCR MOI 30, 60 or 100. The number of gems present in 100 nuclei was quantified 72h post-transduction. (A) Representative images of gems in control human fibroblasts, non-transduced and SMA type I cells transduced at MOI 100. Statistical comparisons can be found in Table S3. Scale bars = 5 µm. (B) Quantification of (A). Error bars represent standard deviation. N=3 biological replicates were collected in each case.

Figure 6: The effect of IDLV_CMV_*Co-hSMN1* transduction on γH2AX foci in SMA type I fibroblasts.

(A) SMA type I fibroblasts were immunostained for γH2AX 72h post-transduction with IDLV_CMV_*Co-hSMN1* at MOI 75. Scale bars = 20 µm in images of wild-type and SMA type I cells, and 50 µm in transduced cells. A view of cells of interest (white dotted line) at increased magnification (lower panel) shows nuclear foci more clearly. (B) The number of foci per cell and (C) percentage of foci-positive cells were quantified. Error bars represent standard deviation. * P<0.05, ** P<0.01. N=3 biological replicates were collected in each case with each technical replicate quantifying at least n=25 cells.

Figure 7: ATM and pATM in wild-type and SMA type I fibroblasts and SMA type I iPSC-derived motor neurons.

Quantification of western blots using protein lysates from wild-type, SMA type I fibroblasts and SMA type I fibroblasts treated with 200 µM hydrogen peroxide (H_2O_2) for 2 hours prior to lysis assessing (A) ATM and (B) pATM levels. (C) Transduction of SMA type I fibroblasts with either IDLV_CMV_*eGFP* or IDLV_CMV_*Co-hSMN1* (both MOI 75) for either 3 or 7 days before harvest and pATM western blot. (D,E) Quantification of ATM and pATM western blots from three independent lines of SMA type I iPSC-derived motor neurons transduced at maturity with IDLV_CMV_*Co-hSMN1* (MOI 75) and harvested 3 days post-transduction. Error bars represent standard deviation. * P<0.05, ** P<0.01, *** P<0.001, **** P<0.0001. N=3 biological replicates were collected in each case. See Supplementary Figure 4 for representative western blot images.

Figure 8: Analysis of SMN levels following *in vivo* neonatal administration of AAV9 vectors expressing *Co-hSMN1.*

814 *Smn*$^{2B/-}$ neonatal (P0) mice were administered AAV9_CAG_*eGFP* or AAV9_CAG_*Co-hSMN1*
815 and their livers (A,B) and spinal cords (C,D) harvested at the symptomatic time-point of P18 for
816 protein analysis. SMN protein levels were normalised to those in wild-type samples in all cases.
817 Error bars represent standard deviation. * $P<0.05$, ** $P<0.01$. Wild-type n=4, untreated *Smn*$^{2B/-}$
818 n=3, *Smn*$^{2B/-}$ + AAV9_CAG_*eGFP* n=5, *Smn*$^{2B/-}$ + AAV9_CAG_*Co-hSMN1* n=5 biological
819 replicates.
820

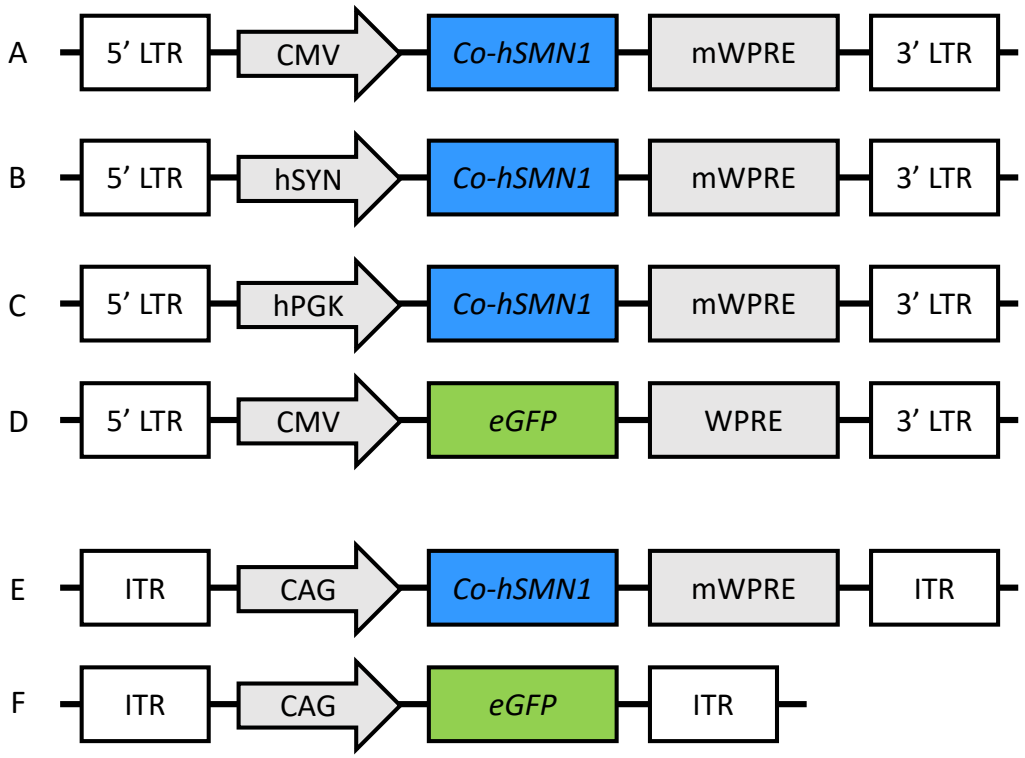
A
5’ LTR
CMV
Co-hSMN1
mWPRE
3’ LTR
B
5’ LTR
hSYN
Co-hSMN1
mWPRE
3’ LTR
C
5’ LTR
hPGK
Co-hSMN1
mWPRE
3’ LTR
D
5’ LTR
CMV
eGFP
WPRE
3’ LTR
E
ITR
CAG
Co-hSMN1
mWPRE
ITR
F
ITR
CAG
eGFP
ITR

A

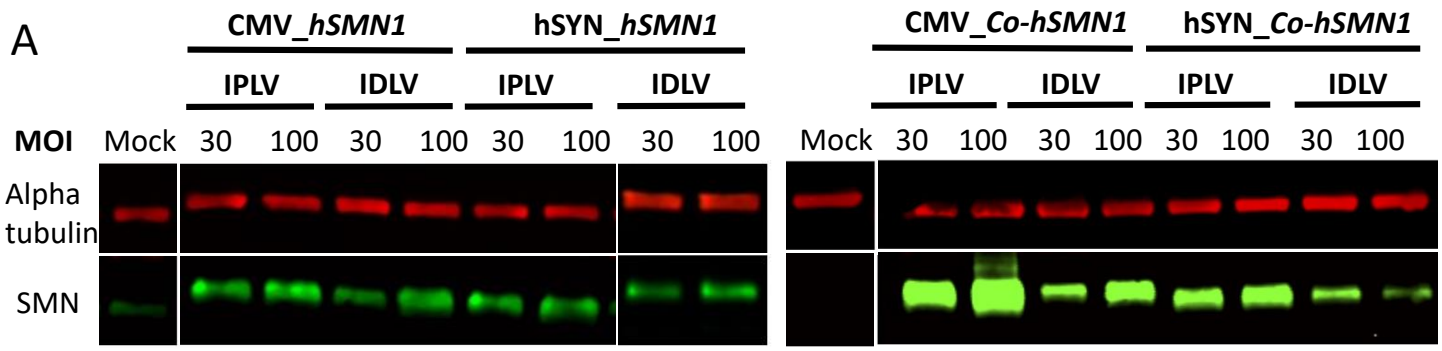
CMV_hSMN1
hSYN_hSMN1
CMV_Co-hSMN1
hSYN_Co-hSMN1
IPLV
IDLV
MOI
Mock
30
100
Alpha tubulin
SMN

B

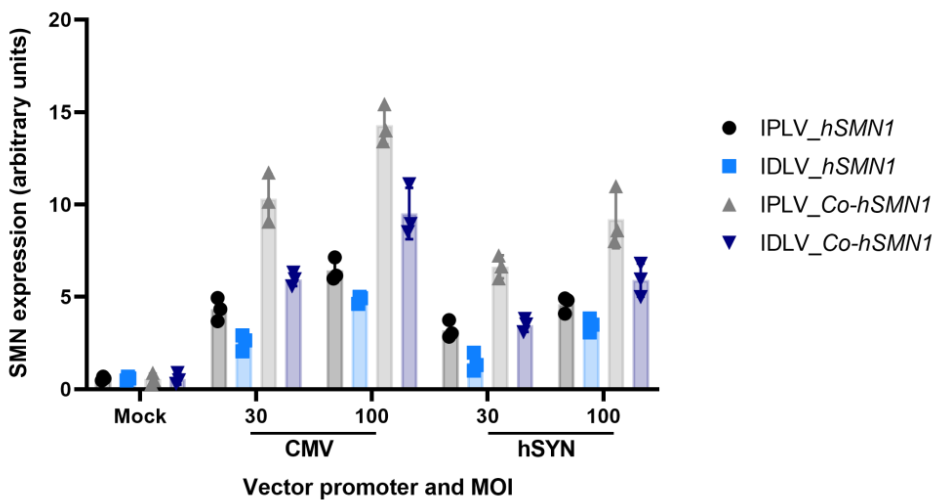
SMN expression (arbitrary units)
20
15
10
5
0
Mock
30
100
CMV
hSYN
Vector promoter and MOI
IPLV_hSMN1
IDLV_hSMN1
IPLV_Co-hSMN1
IDLV_Co-hSMN1

C

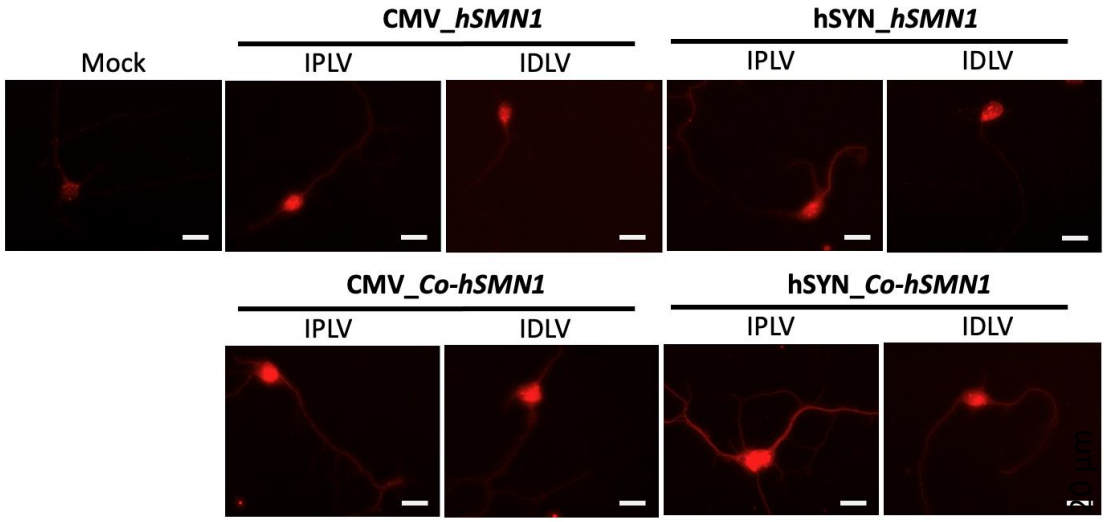
Mock
CMV_hSMN1
hSYN_hSMN1
CMV_Co-hSMN1
hSYN_Co-hSMN1
IPLV
IDLV

D

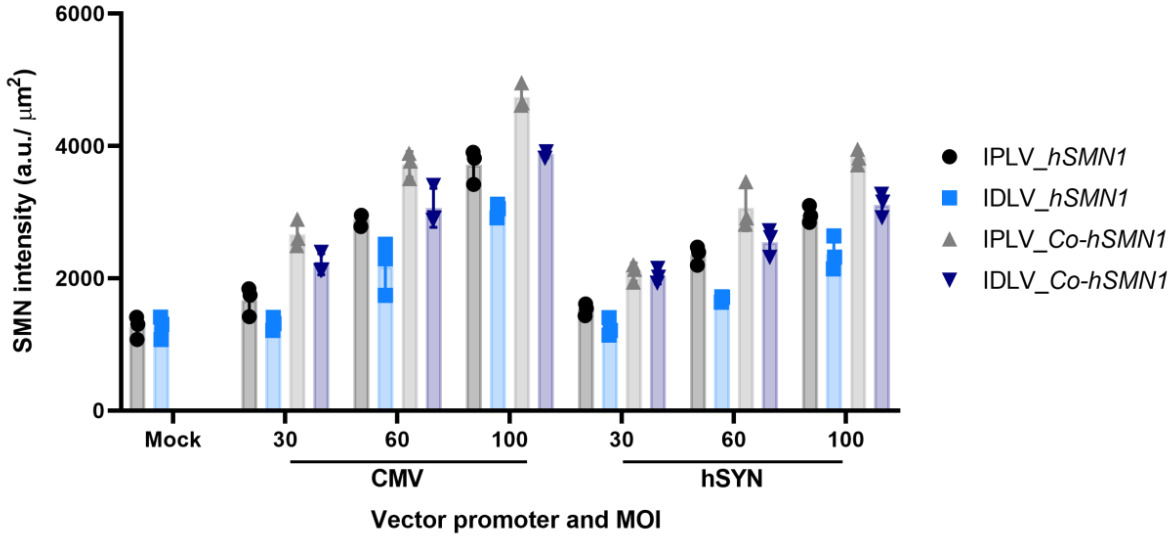
SMN intensity (a.u./ µm²)
6000
4000
2000
0
Mock
30
60
100
CMV
hSYN
Vector promoter and MOI
IPLV_hSMN1
IDLV_hSMN1
IPLV_Co-hSMN1
IDLV_Co-hSMN1

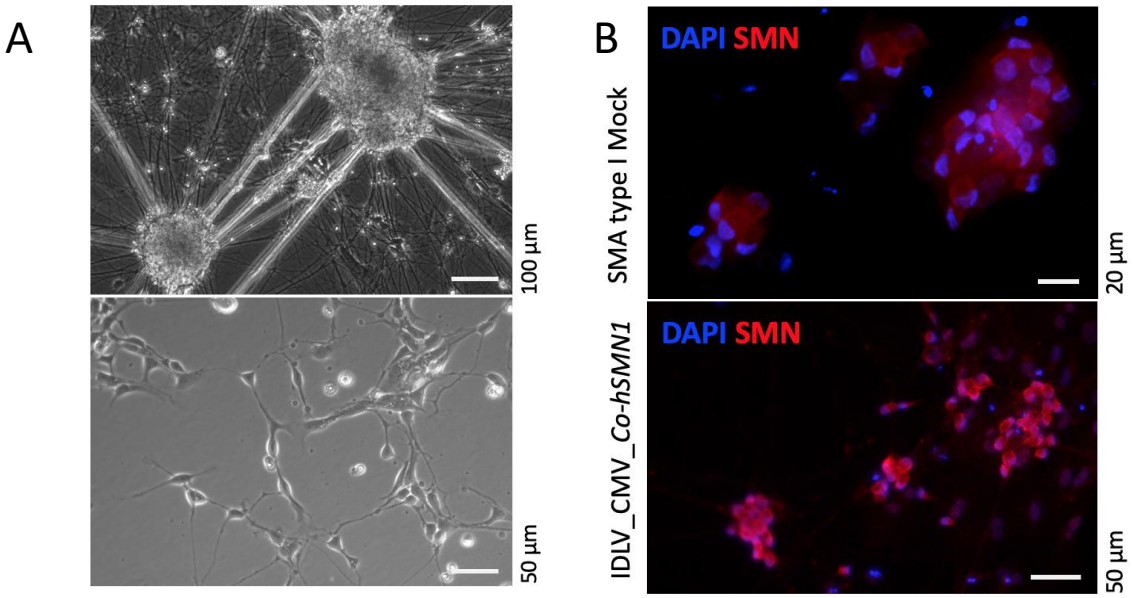
A
100 µm
50 µm
B
DAPI SMN
SMA type I Mock
20 µm
DAPI SMN
IDLV_CMV_Co-hSMN1
50 µm

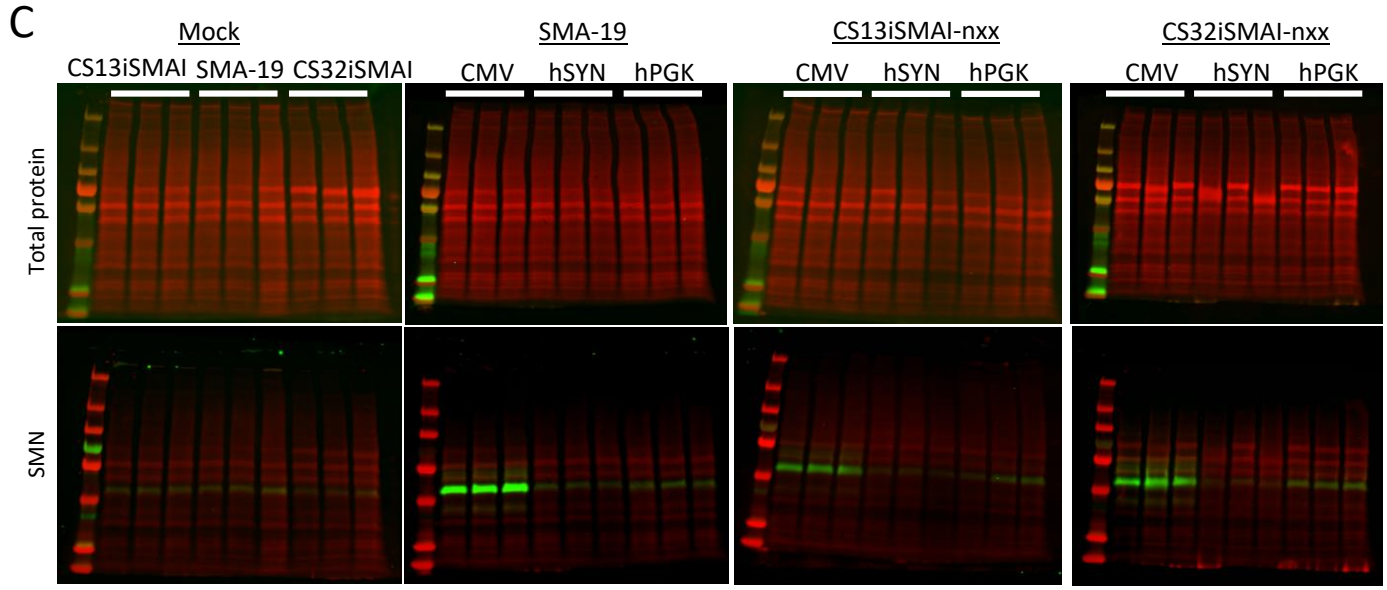
C
Mock
CS13iSMAI SMA-19 CS32iSMAI
SMA-19
CMV hSYN hPGK
CS13iSMAI-nxx
CMV hSYN hPGK
CS32iSMAI-nxx
CMV hSYN hPGK
Total protein
SMN

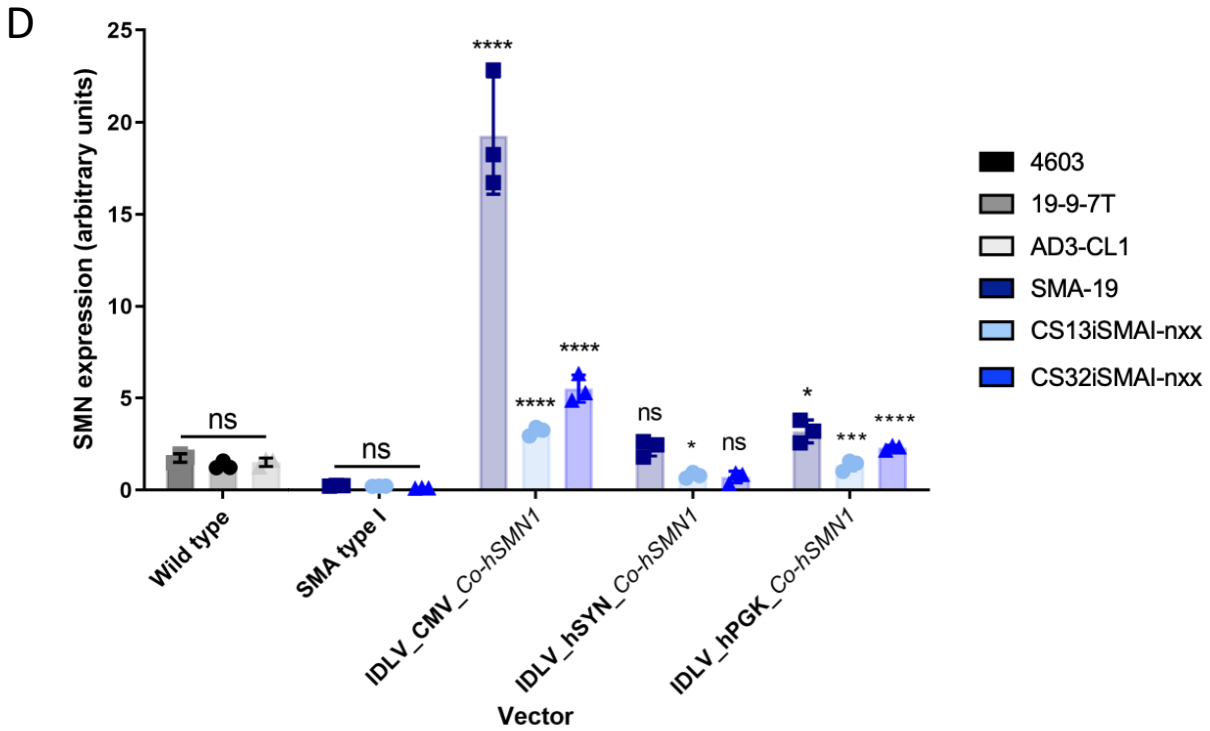
D
SMN expression (arbitrary units)
25
20
15
10
5
0
ns
ns
****
****
****
ns
*
ns
*
***
****
Wild type
SMA type I
IDLV_CMV_Co-hSMN1
IDLV_hSYN_Co-hSMN1
IDLV_hPGK_Co-hSMN1
Vector
4603
19-9-7T
AD3-CL1
SMA-19
CS13iSMAI-nxx
CS32iSMAI-nxx

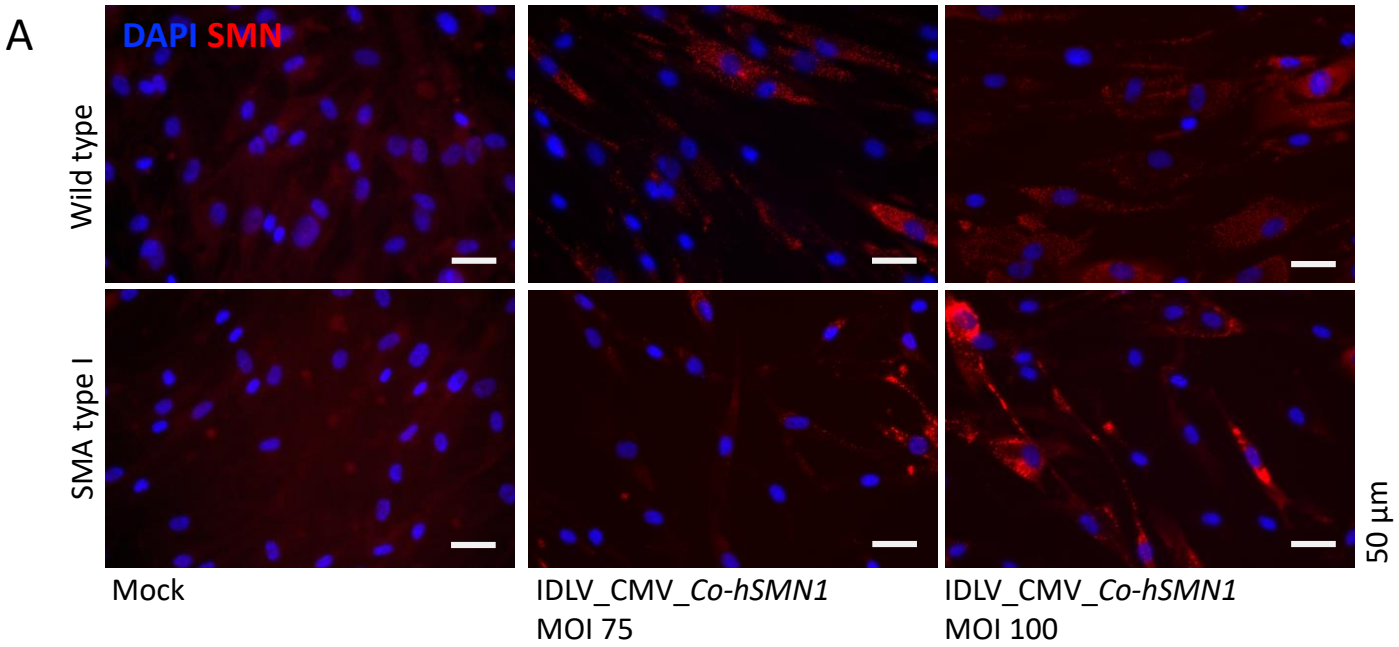
A
DAPI SMN
Wild type
SMA type I
50 µm
Mock
IDLV_CMV_Co-hSMN1
MOI 75
IDLV_CMV_Co-hSMN1
MOI 100

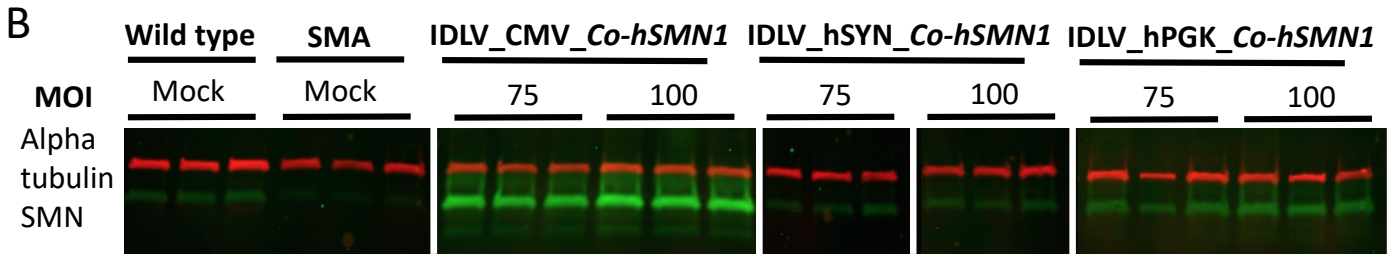
B
Wild type
SMA
IDLV_CMV_Co-hSMN1
IDLV_hSYN_Co-hSMN1
IDLV_hPGK_Co-hSMN1
MOI
Mock
Mock
75
100
75
100
75
100
Alpha tubulin
SMN

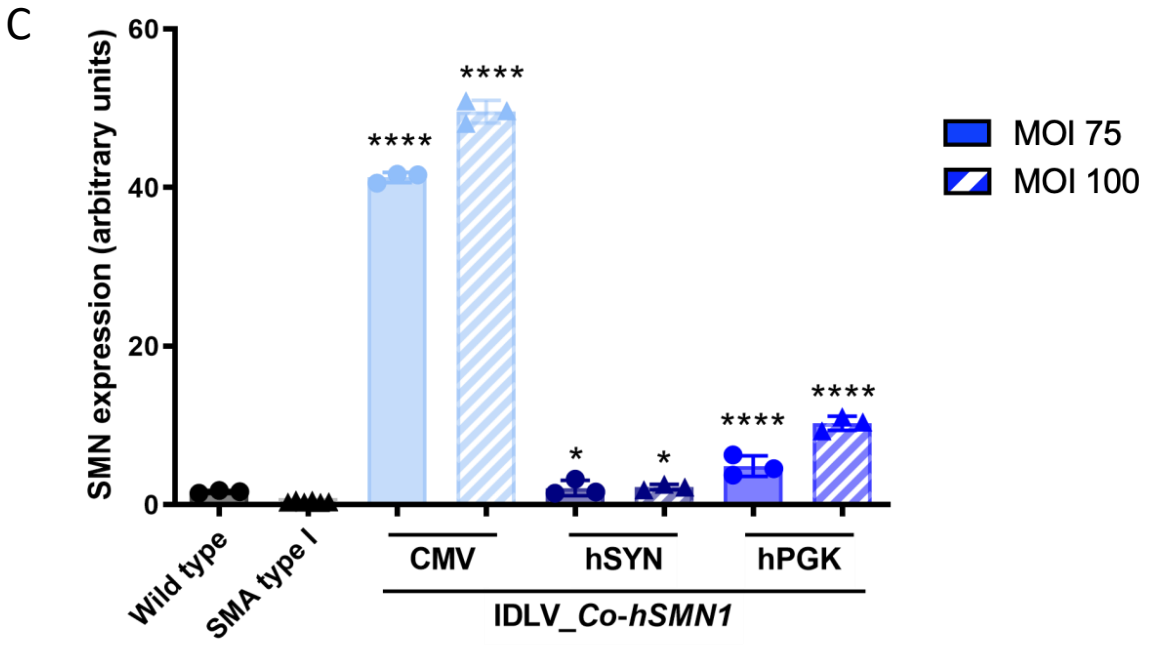
C
SMN expression (arbitrary units)
60
40
20
0
****
****
*
*
****
****
MOI 75
MOI 100
Wild type
SMA type I
CMV
hSYN
hPGK
IDLV_Co-hSMN1

A

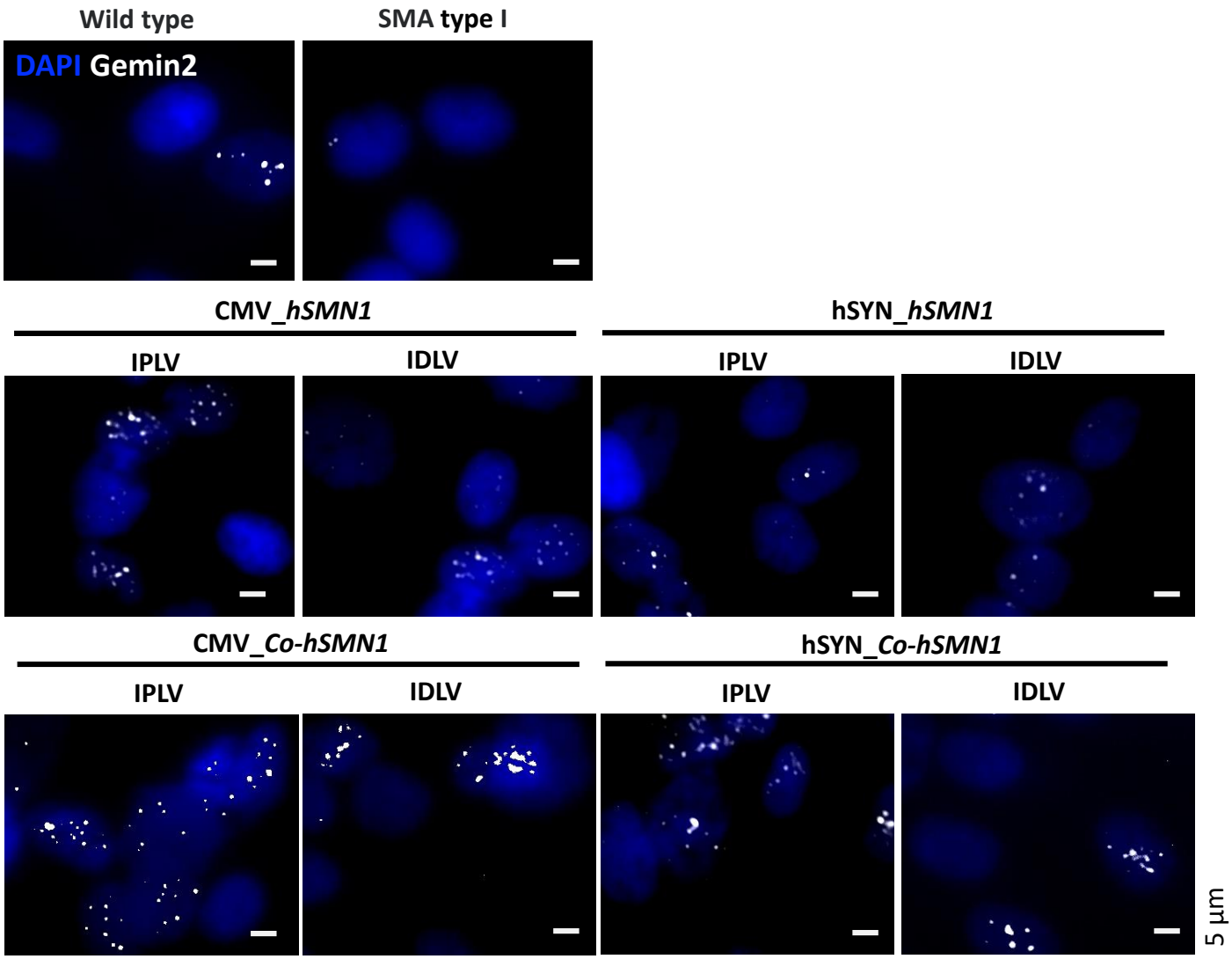
Wild type
SMA type I
DAPI Gemin2
CMV_hSMN1
hSYN_hSMN1
IPLV
IDLV
IPLV
IDLV
CMV_Co-hSMN1
hSYN_Co-hSMN1
IPLV
IDLV
IPLV
IDLV
5 µm

B

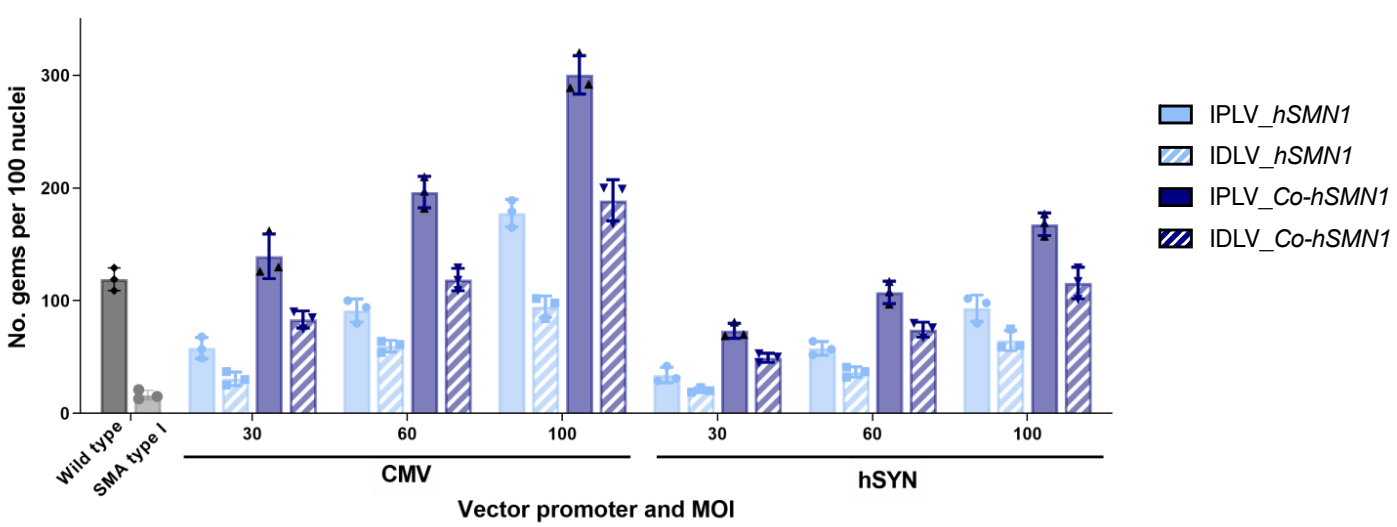
No. gems per 100 nuclei
300
200
100
0
Wild type
SMA type I
30
60
100
30
60
100
CMV
hSYN
Vector promoter and MOI
IPLV_hSMN1
IDLV_hSMN1
IPLV_Co-hSMN1
IDLV_Co-hSMN1

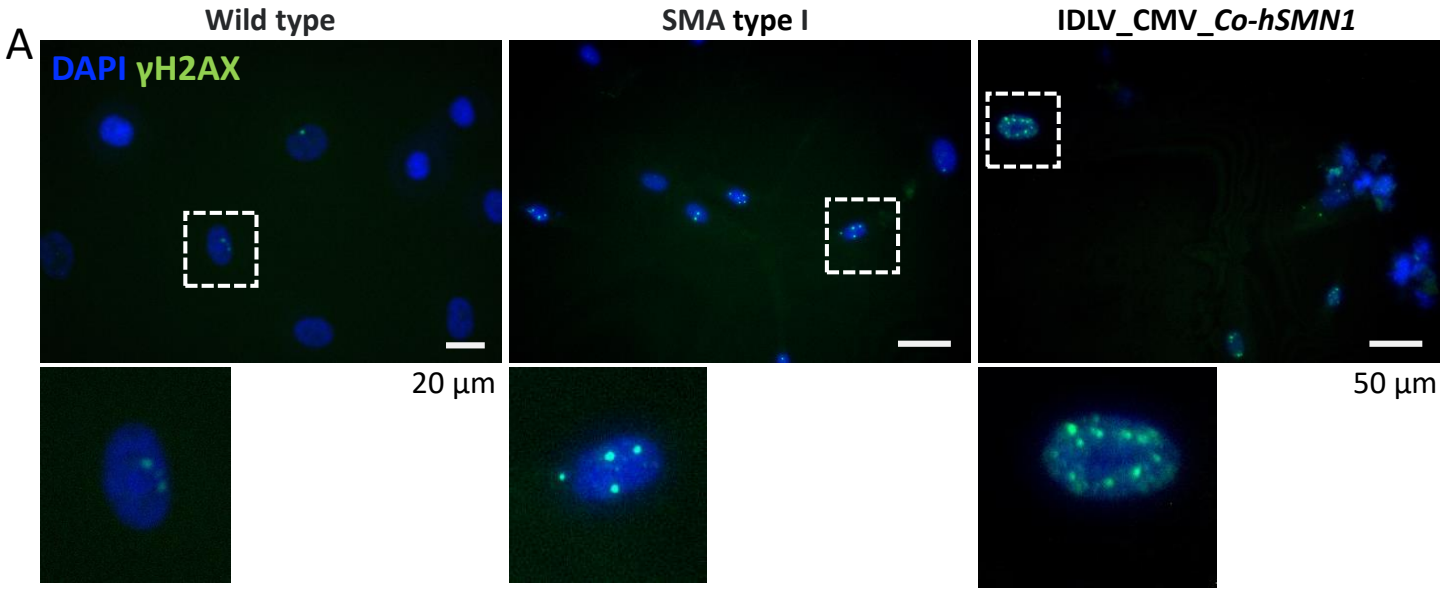
A
Wild type
SMA type I
IDLV_CMV_Co-hSMN1
DAPI γH2AX
20 µm
50 µm

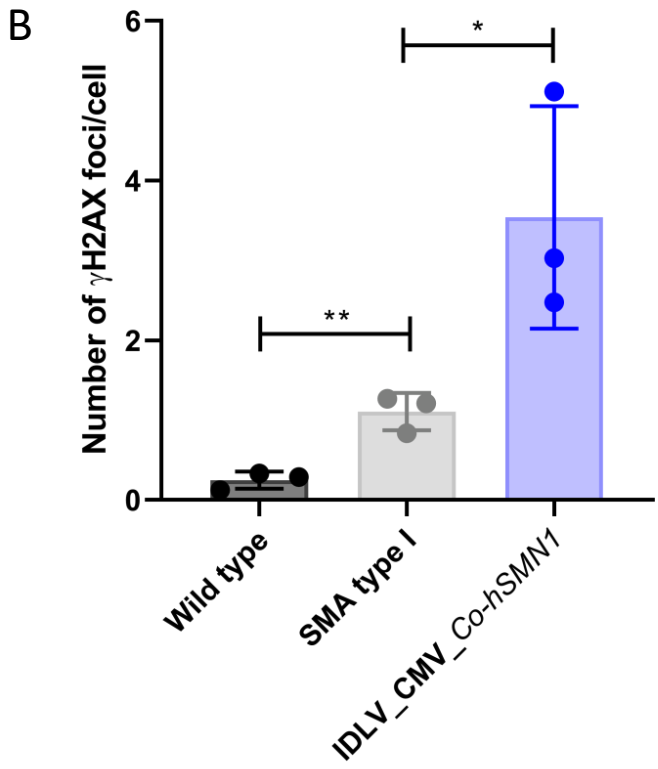
B
Number of γH2AX foci/cell
0
2
4
6
**
*
Wild type
SMA type I
IDLV_CMV_Co-hSMN1

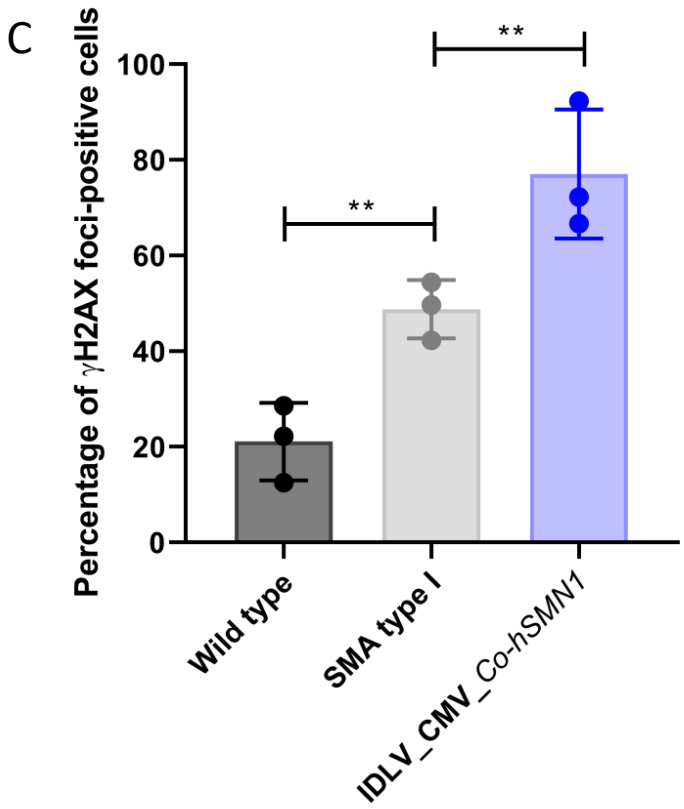
C
Percentage of γH2AX foci-positive cells
0
20
40
60
80
100
**
**
Wild type
SMA type I
IDLV_CMV_Co-hSMN1

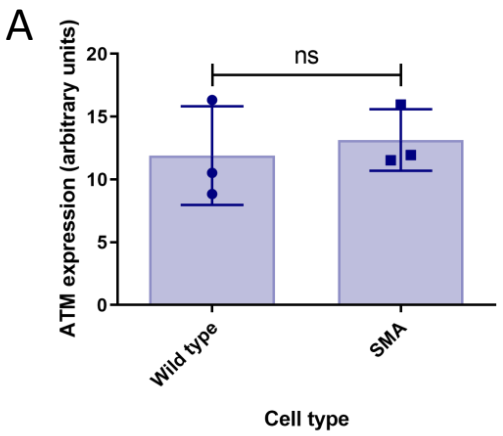
A
ATM expression (arbitrary units)
ns
Wild type
SMA
Cell type

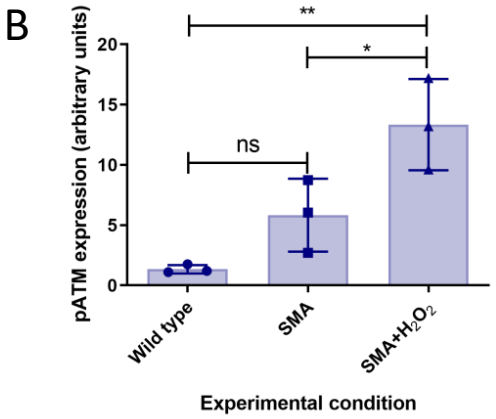
B
pATM expression (arbitrary units)
**
*
ns
Wild type
SMA
SMA+H2O2
Experimental condition

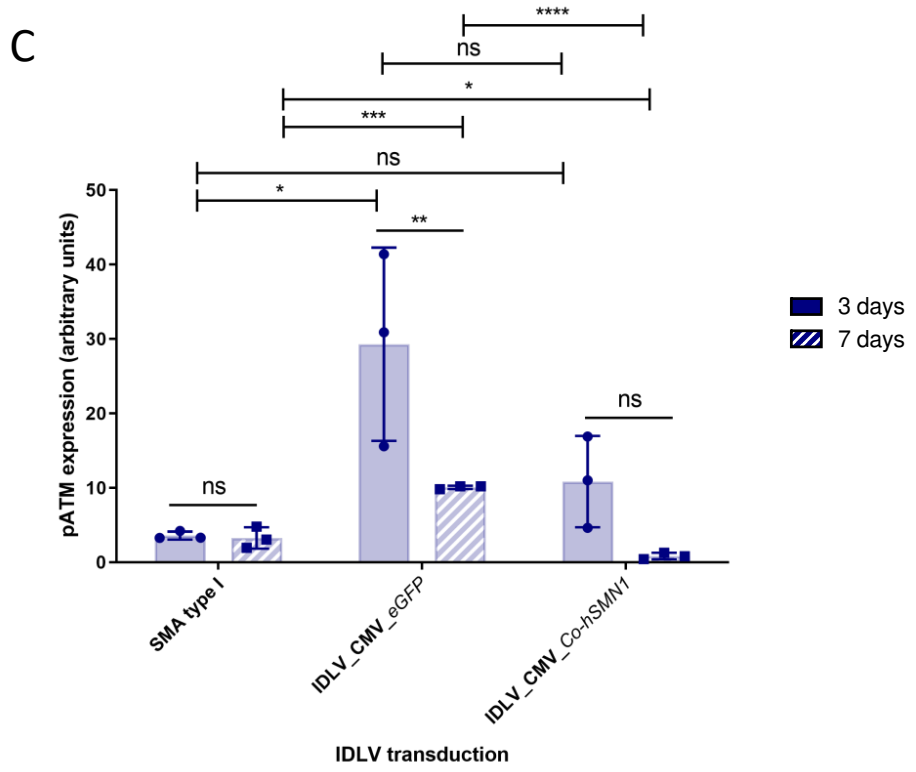
C
pATM expression (arbitrary units)
****
ns
*
***
ns
*
**
ns
ns
SMA type I
IDLV_CMV_eGFP
IDLV_CMV_Co-hSMN1
IDLV transduction
3 days
7 days

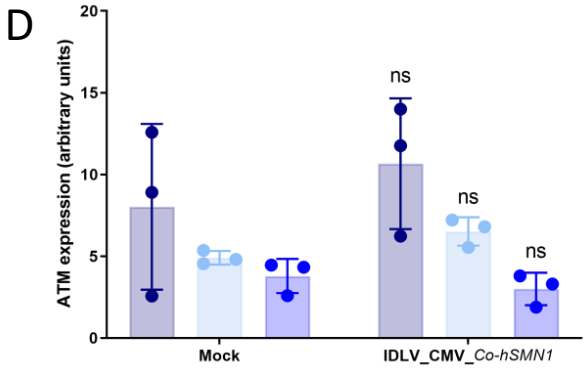
D
ATM expression (arbitrary units)
ns
ns
ns
Mock
IDLV_CMV_Co-hSMN1

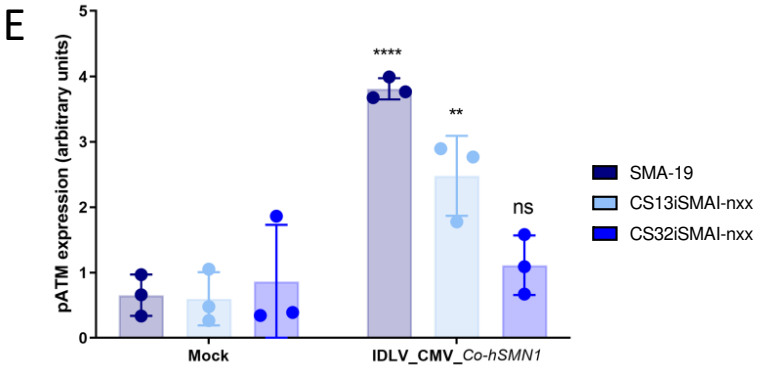
E
pATM expression (arbitrary units)
****
**
ns
Mock
IDLV_CMV_Co-hSMN1
SMA-19
CS13iSMAI-nxx
CS32iSMAI-nxx

A

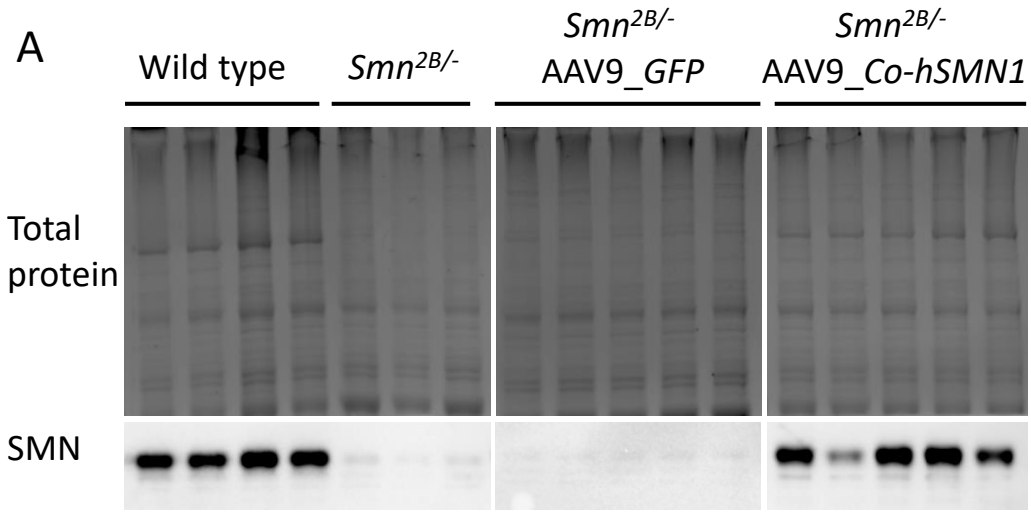
Wild type
Smn2B/-
Smn2B/- AAV9_GFP
Smn2B/- AAV9_Co-hSMN1
Total protein
SMN

B

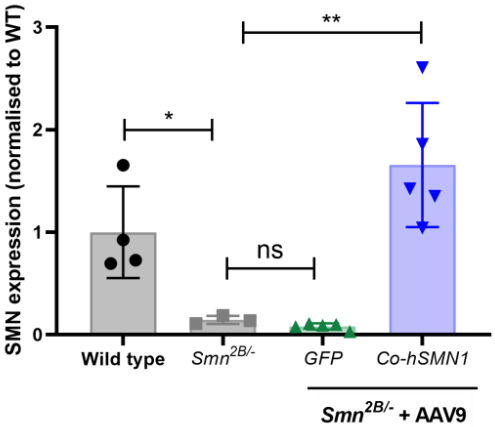
SMN expression (normalised to WT)
3
2
1
0
*
**
ns
Wild type
Smn2B/-
GFP
Co-hSMN1
Smn2B/- + AAV9

C

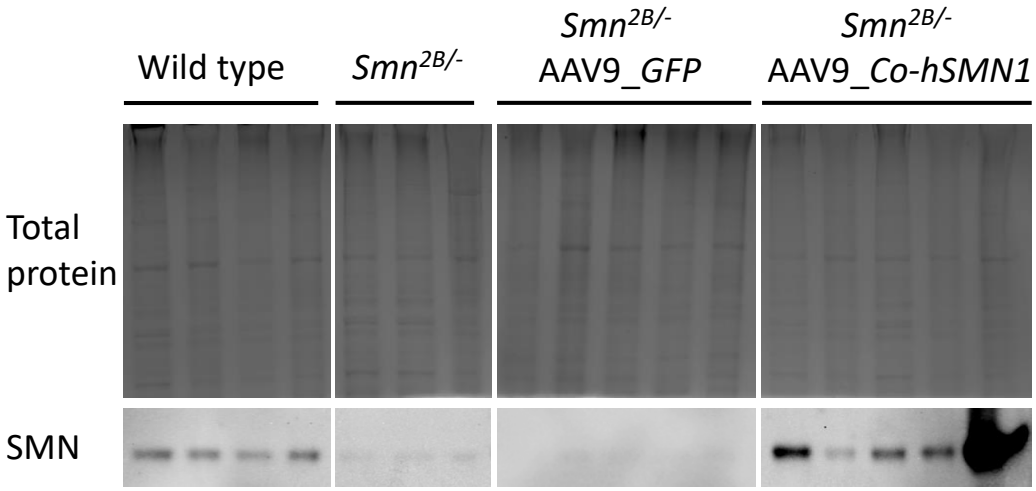
Wild type
Smn2B/-
Smn2B/- AAV9_GFP
Smn2B/- AAV9_Co-hSMN1
Total protein
SMN

D

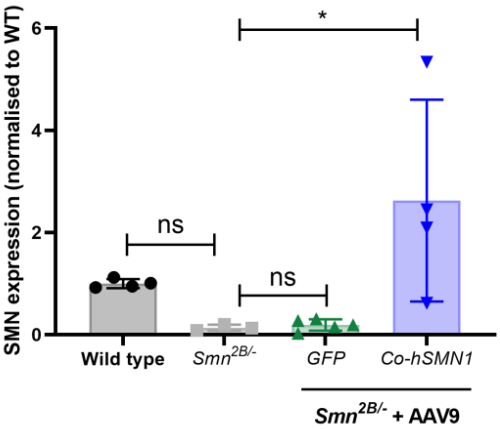
SMN expression (normalised to WT)
6
4
2
0
*
ns
ns
Wild type
Smn2B/-
GFP
Co-hSMN1
Smn2B/- + AAV9

Enhanced expression of the human *Survival motor neuron 1* gene from a codon-optimised cDNA transgene *in vitro* and *in vivo*

Neda A.M. Nafchi[1]*, Ellie M. Chilcott[1]*, Sharon Brown[2,3], Heidi R. Fuller[2,3], Melissa Bowerman[3,4] and Rafael J. Yáñez-Muñoz[1].

[1] AGCTlab.org, Centre of Gene and Cell Therapy, Centre for Biomedical Sciences, Department of Biological Sciences, School of Life Sciences and Environment, Royal Holloway University of London, TW20 0EX, UK.

[2] School of Pharmacy and Bioengineering, Keele University, Staffordshire, ST5 5BG, UK.

[3] Wolfson Centre for Inherited Neuromuscular Disease, TORCH Building, RJAH Orthopaedic Hospital, Oswestry SY10 7AG, UK.

[4] School of Medicine, Keele University, Staffordshire, ST5 5BG UK.

*These authors contributed equally to this work.

Corresponding author:

Prof. Rafael J. Yáñez-Muñoz

Email: rafael.yanez@royalholloway.ac.uk

SUPPLEMENTARY MATERIAL

Supplementary Figure 1: Pairwise alignment of wild-type and *Co-hSMN1* cDNA sequences.

The sequences of the wild-type *SMN1* cDNA (top) and the *Co-hSMN1* cDNA (bottom) open reading frames were aligned, and nucleotide differences highlighted with asterisks.

Supplementary Figure 2: Characterisation of cortical and motor neurons in culture.

(A) 6 day-old mouse cortical neuron cultures were fixed and stained with neuron marker (NeuN). Nuclei were stained blue with DAPI. (B) 72-hours post-seeding, rat motor neurons were fixed and immunostained for a common motor neuronal marker (ChAT) to confirm motor neuron identity. Scale bars = 100 μm.

Supplementary Figure 3: Characterisation of iPSC-derived motor neurons.

Representative images of motor neuron cells at different stages of the differentiation protocol. (A) OLIG2-positive (green) motor neuron progenitors at day 16 of differentiation. (B-D) Mature motor neurons express (B) SMI-32 (red) and βIII-tubulin (green), (C) HB9 (red) and (D) ChAT (green). All counterstained with DAPI (blue).

Supplementary Figure 4: Determining *SMN* transcript origin and SMN protein levels in iPSC-derived MNs.

An RT-PCR was performed using primers to amplify a region between exons 6-8 of the *SMN* genes in iPSC-derived MNs. -RT = minus reverse transcriptase control reaction. (A) Full length *SMN* (*FL-SMN*) products (504bp) and *SMNΔ7* transcripts (450bp) are shown. (B) Two control gene products (GAPDH: 184bp and β-actin: 295bp) were also amplified. The same lane order is present in all gels. (C) The two bands seen at 504 and 450bp in (A) were excised separately and purified. PCR amplicons were digested with *Dde*I for 2 hours before running digested products on a second gel to reveal diagnostic *Dde*I restriction site present only in *SMN2*

transcripts. Cleavage products: *FL-SMN2* (504bp) = 382 and 122bp, *SMN2Δ7* (450bp) = 328 and 122bp. (D,E) SMA type I MNs show 18-fold (P<0.0001) less SMN protein than wild type MNs at day 31 of differentiation. N=3 biological replicates were collected for each line.

Supplementary Figure 5: Representative western blot images of ATM and pATM levels in SMA type I fibroblasts (top and middle panels) and iPSC-derived motor neurons (bottom panel).

Quantification can be found in Figure 7.

Supplementary Figure 6: Immunofluorescence staining pattern of cleaved caspase 3 and γH2AX in wild-type, SMA type I fibroblasts and SMA type I fibroblasts transduced with IDLV_CMV_*Co-hSMN1.*

Fibroblasts were immunostained against cleaved caspase 3 before the staining pattern was quantified. (A) A scoring system was designed to delineate levels of expression: 0 = no signal, 1 = less than 5 foci, 2 = more than 5 foci, 3 = light, diffuse staining, 4 = strong, diffuse staining throughout whole nucleus, or very strong expression in a concentrated area. Examples of nuclei representative of scores 1-4 are shown. (B) Values for each cleaved caspase 3 score as a percentage of total cells in each replicate were calculated and an unpaired, one-tailed t-test between wild-type and SMA (average 19 and 37 cells per replicate, respectively), at each score was conducted (0: P=0.0006, 1: P=0.0472, 2: P=0.0451, 3: P=0.4565, 4: P=0.1613). (C) The percentage of total SMA type I cells exhibiting each score was calculated, but large variation is seen in both mock and transduced samples. At least 30 cells per replicate were scored for each condition (total n=107 mock transduced cells, n=115 transduced cells). Significance was assessed at each score by unpaired, two-tailed t-tests (0: P=0.1751, 1: P=0.8194, 2: P=0.9031, 3: P=0.5228, 4: P=0.8709).

Supplementary Table 1: Comparison of SMN protein production from all vectors in primary mouse cortical neurons.

One-way ANOVA and Bonferroni's post-hoc test were used to determine significant differences in western data from transduced mouse cortical neurons (shown in Figure 2A-B). The data compare types of vectors, transgenes and promoters on protein production. Additionally, data were analysed to determine whether there was a dose-dependent increase within each group. Values represent mean ± SEM. * $P<0.05$, ** $P<0.01$, *** $P<0.001$. N=3 biological replicates were collected in each case.

Supplementary Table 2: Comparison of SMN protein production from all vectors in primary rat motor neurons.

One-way ANOVA and Bonferroni's post-hoc test were used to determine significant differences in immunofluorescence data from transduced primary rat motor neurons (shown in Figure 2C-D). Data compare types of vectors, transgenes and promoters on protein production. Additionally, data were analysed to determine whether there was a dose-dependent increase within each group. Values represent mean ± SEM. * $P<0.05$, ** $P<0.01$, *** $P<0.001$. N=3 biological replicates were collected in each case.

Supplementary Table 3: Comparison of gem restoration by all vectors in SMA type I fibroblasts.

One-way ANOVA and Bonferroni's post-hoc test was used to determine significant differences in type I SMA fibroblast populations (shown in Figure 5). The analysed data show the effect of different parameters such as lentiviral vector configuration, transgene and promoter, on gem restoration. In addition, data were analysed to determine whether there were dose-dependent

increases within each promoter group. Values represent mean ± SEM. * $P<0.05$, ** $P<0.01$, *** $P<0.001$. N=3 biological replicates were collected in each case.

Supplementary Figure S1

```
atggcgatgagcagcggcggcagtggtggcggcgtcccggagcaggaggattccgtgctgttccggcgcggcacaggccagagcgatgattctgacattt   100
atggccatgagcagcggcggctctggcggcggagtgcccgagcaggaagatagcgtcctgttcagacggggcaccggccagagcgacgacagcgacatct   100
     *               **   *     *  *  *        *   **   *        *  *     *           *  ****     *

gggatgatacagcactgataaaagcatatgataaagctgtggcttcatttaagcatgctctaaagaatggtgacatttgtgaaacttcgggtaaaccaaa   200
gggacgacaccgccctgatcaaggcctacgacaaggccgtggccagcttcaagcacgccctgaagaacggcgacatctgcgagacaagcggcaagcccaa   200
    *  *  *  *     *  *  *  *  *  *  *     ****  *     *  *  *     *  *     *  *  *    **  *  *  *

aaccacacctaaaagaaaacctgctaagaagaataaaagccaaaagaagaatactgcagcttccttacaacagtggaaagttggggacaaatgttctgcc   300
gaccacccccaagcggaagcccgccaagaagaacaagagccagaagaagaacaccgccgccagcctccagcagtggaaagtgggcgacaagtgcagcgcc   300
*     *  *  ** *  *  *  *        *  *     *        *  *  *  ***   *                *  *     *  ****

atttggtcagaagacggttgcatttacccagctaccattgcttcaattgattttaagagagaaacctgtgttgtggtttacactggatatggaaatagag   400
atttggagcgaggacggctgcatctaccccgccacaatcgccagcatcgacttcaagcgggaaacctgcgtggtggtgtacaccggctacggcaacagag   400
      ***        *    *     *  *     *  ****  *  *  *   * *        *  *     *     *  *  *  *  *

aggagcaaaatctgtccgatctactttccccaatctgtgaagtagctaataatatagaacaaaatgctcaagagaatgaaaatgaaagccaagtttcaac   500
aggaacagaacctgagcgacctgctgagccccatctgcgaggtggccaacaacatcgagcagaacgcccaggaaaacgagaacgagagccaggtgtccac   500
    *  *  *   **   *  *  ***   *     *  *  *  *  *  *  *  *  *  *  *  *  *  *  *     *  *  *

agatgaaagtgagaactccaggtctcctggaaataaatcagataacatcaagcccaaatctgctccatggaactcttttctccctccaccaccccccatg   600
cgacgagagcgagaacagcagaagccccggcaacaagagcgacaacatcaagcctaagagcgccccctggaacagcttcctgccccctcccccaccaatg   600
*  *  *        **  ****  *  *  *  ****  *           *  ****  *  *      ***  *  *  *  *  *  *  *

ccagggccaagactgggaccaggaaagccaggtctaaaattcaatggcccaccaccgccaccgccaccaccaccaccccacttactatcatgctggctgc   700
cctggccctagactgggccctggcaagcccggcctgaagttcaacggccctcccccccacctccaccaccccctccacatctgctgagctgctggctgc   700
  *  *  *        *  *  *     *  *  *  *     *     *  *  *     *        *  *  *  ** *  ****

ctccatttccttctggaccaccaataattcccccaccacctcccatatgtccagattctcttgatgatgctgatgctttgggaagtatgttaatttcatg   800
ccccattccccagcggccctcccatcattccccctccaccccccatctgccccgacagcctggatgatgccgacgccctgggcagcatgctgatcagctg   800
       *  **** *  *  *  *              *     *  *  *  ****  *        *  *  **    ** *   * *  ****

gtacatgagtggctatcatactggctattatatgggtttcagacaaaatcaaaaagaaggaaggtgctcacattccttaaattaa   885
gtacatgagcggctaccacacaggctactacatgggcttccggcagaaccagaaagagggccgctgctcccacagcctgaactga   885
         *     *  *  *     *  *     *   * *  *  *  *     *  ** *     *  *** * *   **
```

Supplementary Figure S2

A

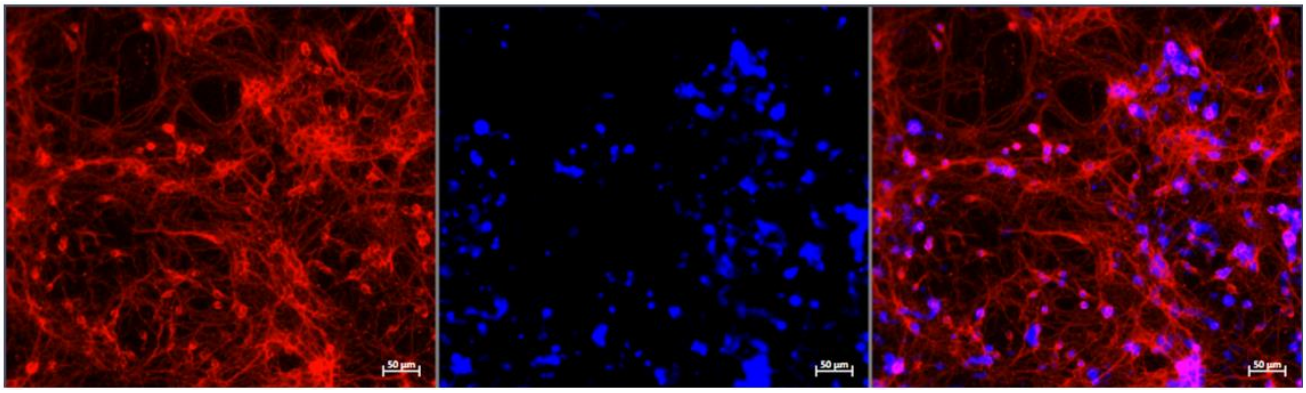

NeuN DAPI Merge

B

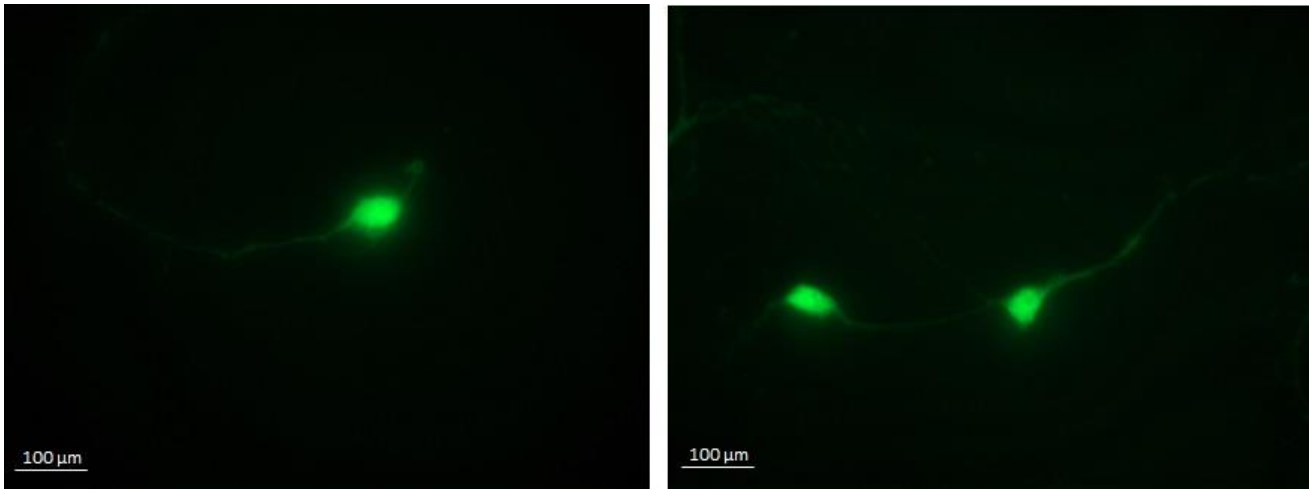

ChAT

Supplementary Figure S3

A

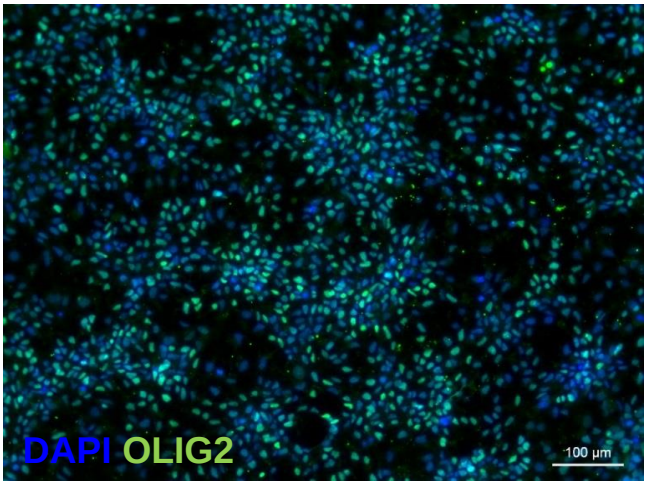

B

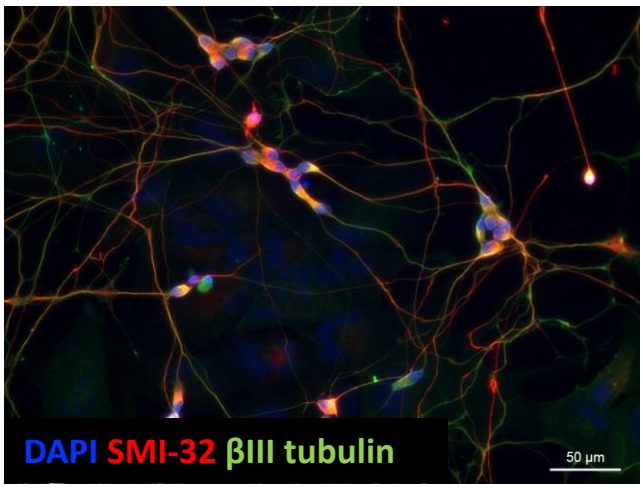

C

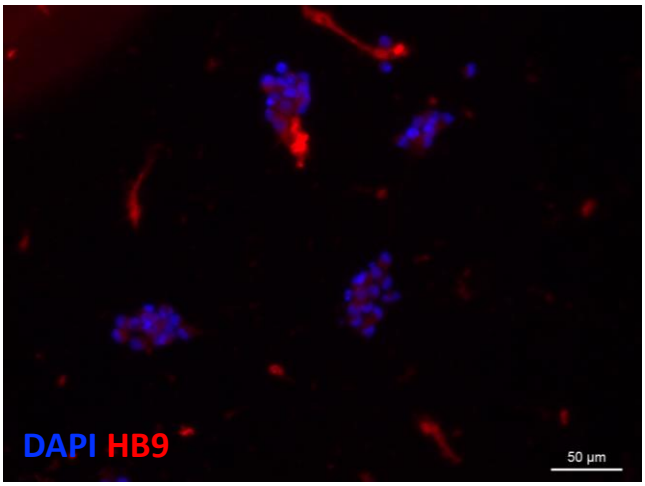

D

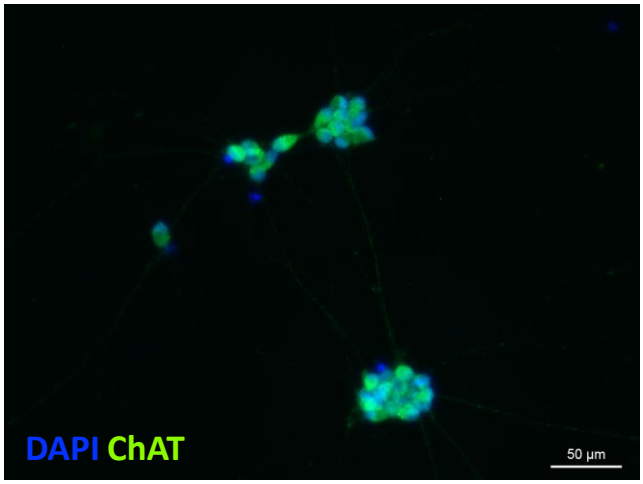

Supplementary Figure S4

A

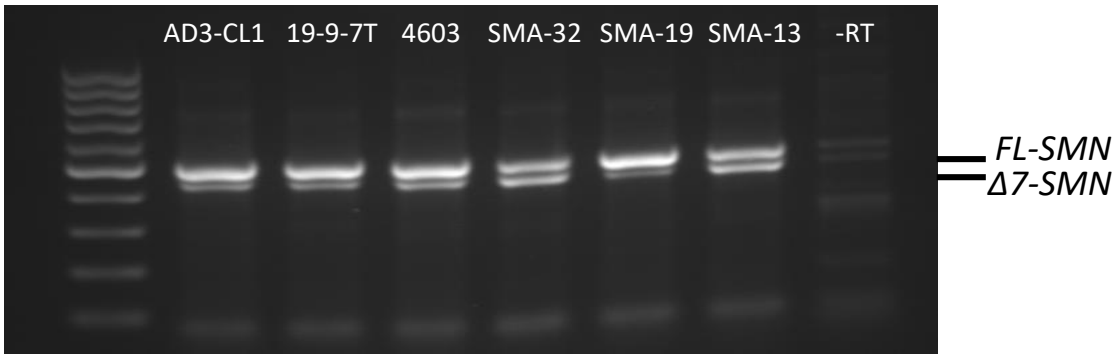

B

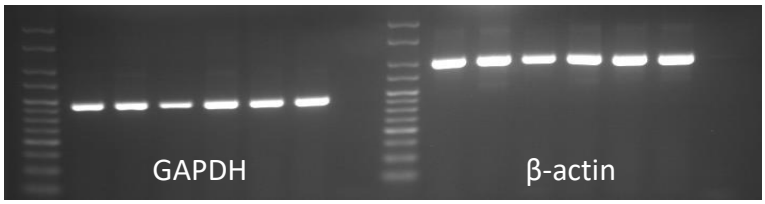

C

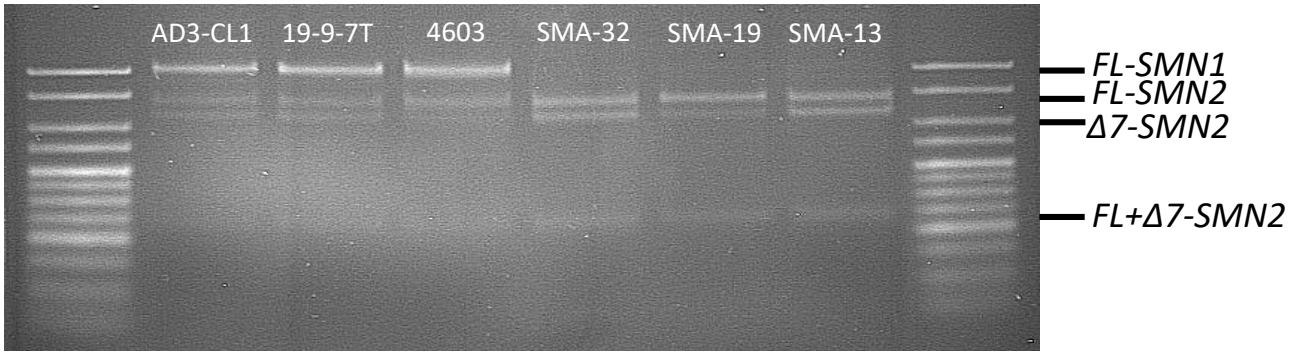

D

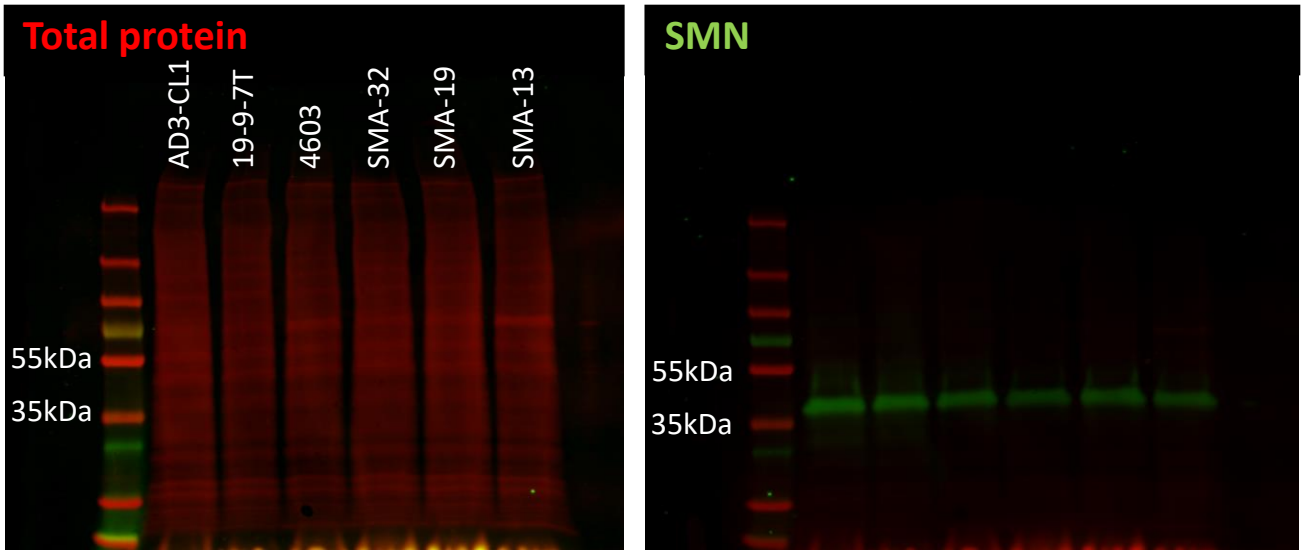

E

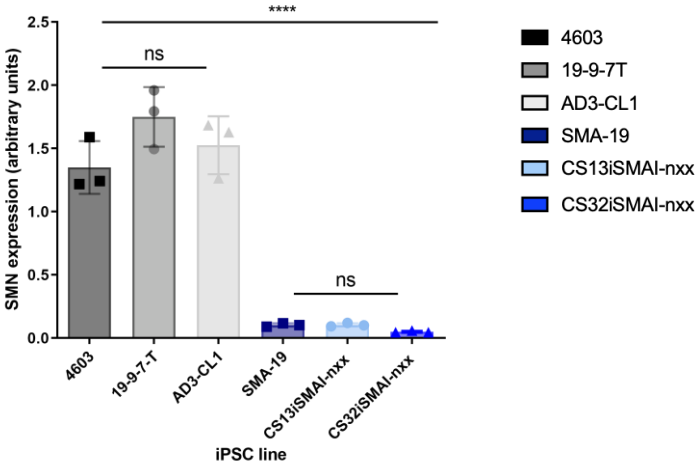

Supplementary Figure S5

A

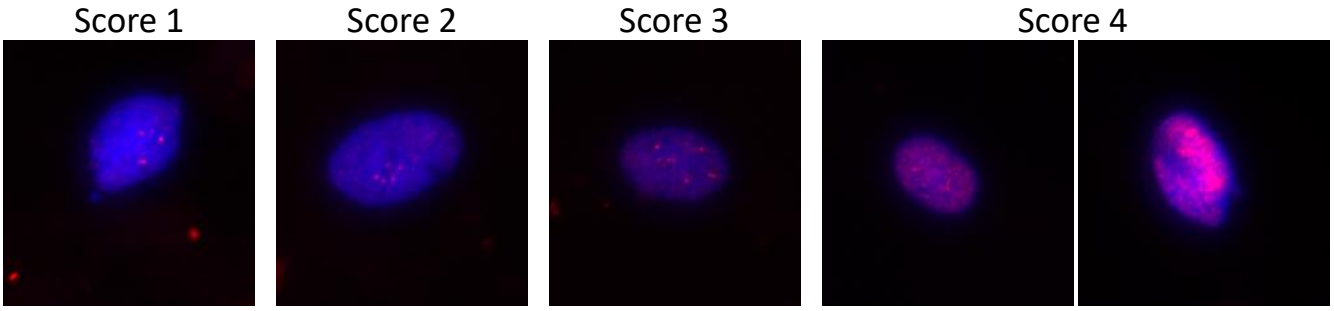

B

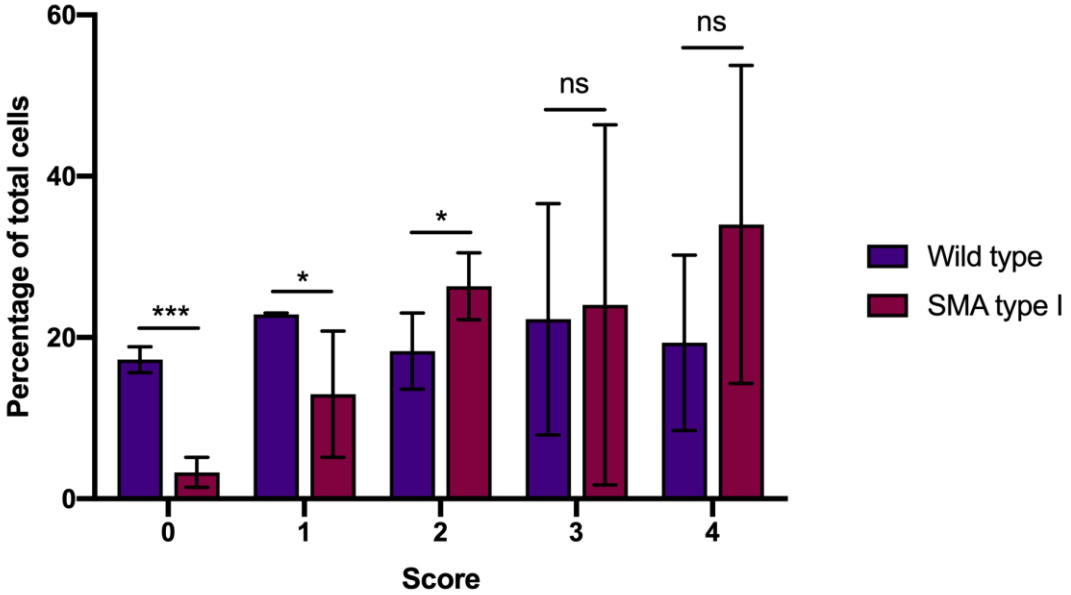

C

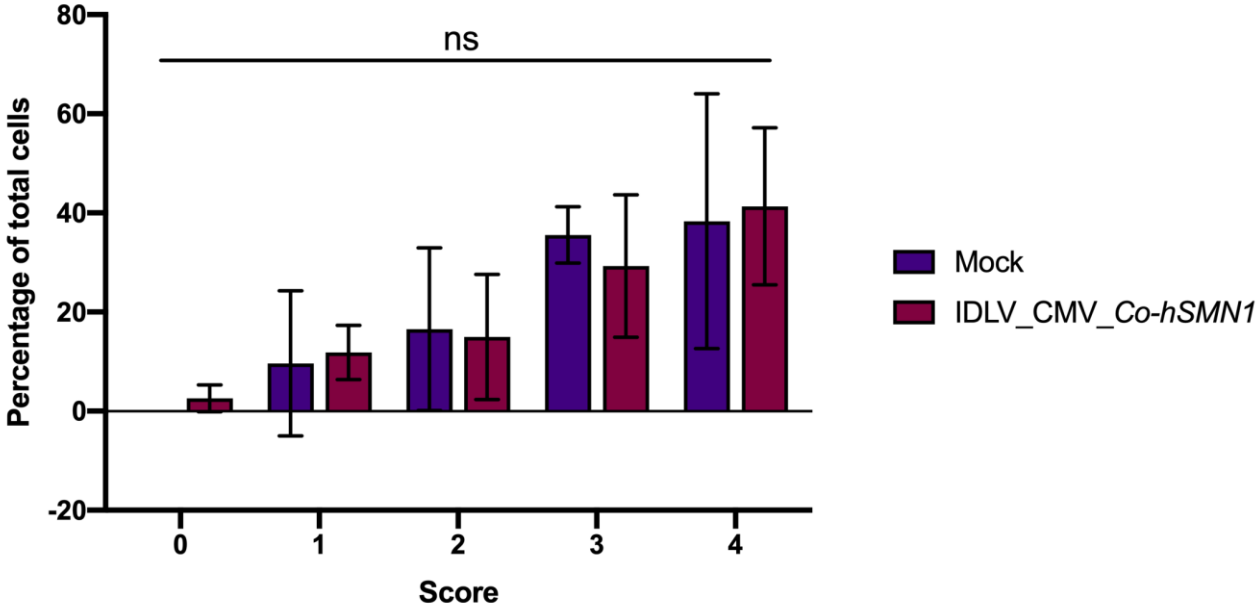

Supplementary Figure S6

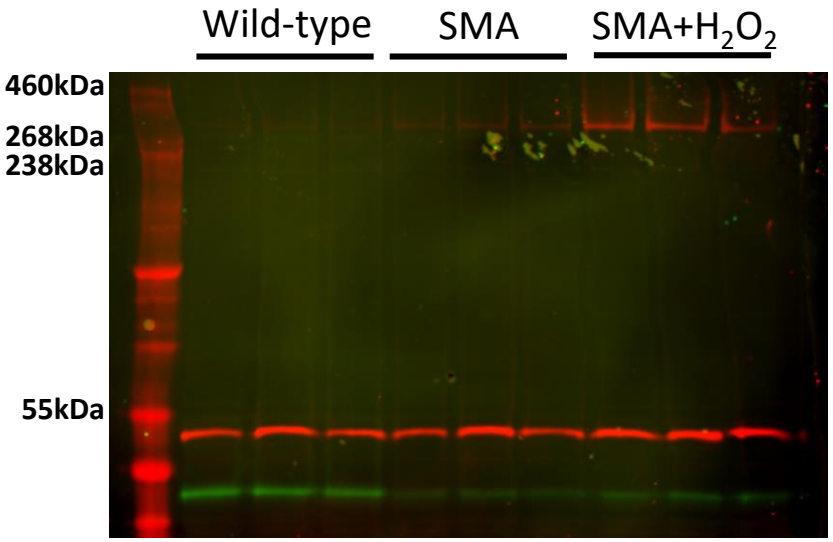

pATM (350kDa) Alpha tubulin (55kDa) SMN (38kDa)

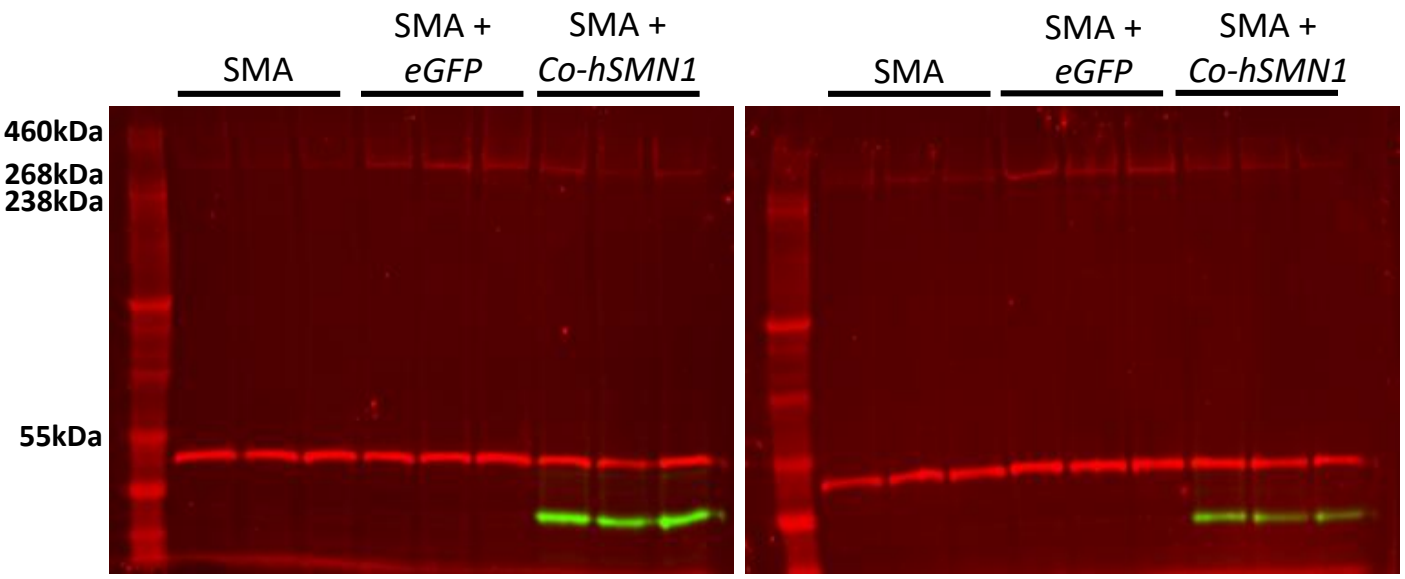

pATM (350kDa) Alpha tubulin (55kDa) SMN (38kDa)

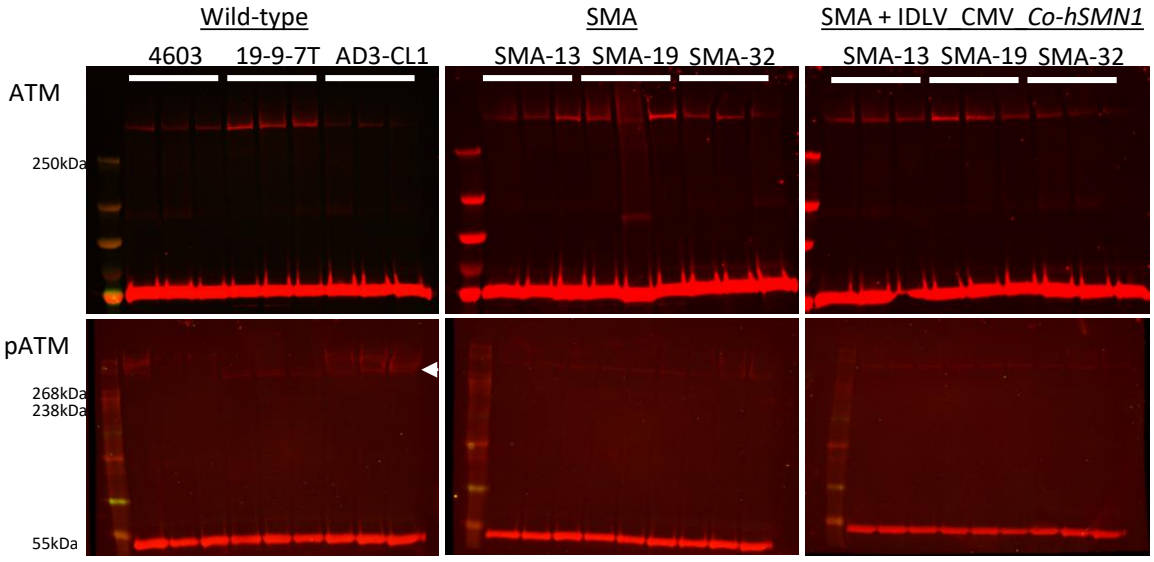

Alpha tubulin (55kDa) ATM and pATM (350kDa)

Supplementary Table S1

Transgene	Promoter	Vector	Transgene	*hSMN1*								*Co-hSMN1*							
			Promoter	CMV				hSYN				CMV				hSYN			
			Vector	IPLV		IDLV		IPLV		IDLV		IPLV		IDLV		IPLV		IDLV	
			MOI	30	100	30	100	30	100	30	100	30	100	30	100	30	100	30	100
hSMN1	CMV	IPLV	30		***	**		*					**	***		**			
			100				**		**						***		***		
		IDLV	30				***			*					**			*	
			100								*								**
	hSYN	IPLV	30						*	**							*	**	
			100								*								**
		IDLV	30								***								*
			100																
Co-hSMN1	CMV	IPLV	30	***															
			100		***														
		IDLV	30			***													
			100				***												
	hSYN	IPLV	30					***											
			100						***										
		IDLV	30							*									
			100								**								

	Dose-dependent increase		CMV VS hSYN		IPLV VS IDLV		*hSMN1* VS Co-*hSMN1*

Supplementary Table S2

Transgene	Promoter	Vector	Transgene	*hSMN1*												*Co-hSMN1*											
			Promoter	CMV						hSYN						CMV						hSYN					
			Vector	IPLV				IDLV		IPLV			IDLV			IPLV			IDLV			IPLV			IDLV		
			MOI	30	60	100	30	60	100	30	60	100	30	60	100	30	60	100	30	60	100	30	60	100	30	60	100
hSMN1	CMV	IPLV	30		***	***	ns			ns						***											
			60			**		***			*						**										
			100						***			***						***									
		IDLV	30					*	***				ns						**								
			60						*					*						**							
			100												**						**						
	hSYN	IPLV	30								***	***	ns									*					
			60									**		**									**				
			100												**									**			
		IDLV	30											*	***										**		
			60												**											***	
			100																								**
Co-hSMN1	CMV	IPLV	30														**	***	ns			*					
			60															**		**			**				
			100																		***			***			
		IDLV	30																	**	***				ns		
			60																		**					*	
			100																								***
	hSYN	IPLV	30																				**	***	ns		
			60																					*		*	
			100																								***
		IDLV	30																							*	***
			60																								*
			100																								

	Dose-dependent increase		CMV VS hSYN		IPLV VS IDLV		*hSMN1* VS Co-*hSMN1*

Supplementary Table S3

Transgene	Promoter	Vector	Transgene	*hSMN1*												*Co-hSMN1*											
			Promoter	CMV						hSYN						CMV						hSYN					
			Vector	IPLV			IDLV			IPLV			IDLV			IPLV			IDLV			IPLV			IDLV		
			MOI	30	60	100	30	60	100	30	60	100	30	60	100	30	60	100	30	60	100	30	60	100	30	60	100
hSMN1	CMV	IPLV	30		*	***	*			ns						***											
			60			**		**			**						***										
			100						***			***						***									
		IDLV	30					**	***				ns						***								
			60						**					ns						***							
			100												*						***						
	hSYN	IPLV	30								*	***	ns									**					
			60									**		ns									***				
			100												*									***			
		IDLV	30											*	***										*		
			60												**											**	
			100																								***
Co-hSMN1	CMV	IPLV	30														*	***	***			***					
			60															***		***			***				
			100																		***			***			
		IDLV	30																	*	***				**		
			60																		**					***	
			100																								***
	hSYN	IPLV	30																				*	***	ns		
			60																					***		**	
			100																								***
		IDLV	30																							*	***
			60																								**
			100																								

	Dose-dependent increase		CMV VS hSYN		IPLV VS IDLV		*hSMN1* VS Co-*hSMN1*